Stem Cell Reports
Resource
OPEN ACCESS

# Small-Molecule-Driven Hepatocyte Differentiation of Human Pluripotent Stem Cells

Richard Siller,[1,4] Sebastian Greenhough,[1,4] Elena Naumovska,[1] and Gareth J. Sullivan[1,2,3,*]
[1]Department of Biochemistry, Faculty of Medicine, Institute of Basic Medical Sciences, University of Oslo, PO Box 1112 Blindern, 0317 Oslo, Norway
[2]Norwegian Center for Stem Cell Research, PO Box 1112 Blindern, 0317 Oslo, Norway
[3]Institute of Immunology, Oslo University Hospital-Rikshospitalet, PO Box 4950 Nydalen, Oslo 0424, Norway
[4]Co-first author
*Correspondence: gareth.sullivan@medisin.uio.no
http://dx.doi.org/10.1016/j.stemcr.2015.04.001


## SUMMARY

The differentiation of pluripotent stem cells to hepatocytes is well established, yet current methods suffer from several drawbacks. These include a lack of definition and reproducibility, which in part stems from continued reliance on recombinant growth factors. This has remained a stumbling block for the translation of the technology into industry and the clinic for reasons associated with cost and quality. We have devised a growth-factor-free protocol that relies on small molecules to differentiate human pluripotent stem cells toward a hepatic phenotype. The procedure can efficiently direct both human embryonic stem cells and induced pluripotent stem cells to hepatocyte-like cells. The final population of cells demonstrates marker expression at the transcriptional and protein levels, as well as key hepatic functions such as serum protein production, glycogen storage, and cytochrome P450 activity.

## INTRODUCTION

Human embryonic stem cells (hESCs) and induced pluripotent stem cells (hiPSCs) offer a potentially limitless source of cells for industrial and clinical translation, and the ever-advancing field of cellular reprogramming has redefined the limits of cell plasticity (Taylor et al., 2010). Meanwhile, cell culture and production technologies are rapidly improving, and the first instances of pluripotent-cell-derived therapies have entered clinical trials (Schwartz et al., 2012).

Amidst this broadening field, hepatocyte generation is gathering interest with industrial and clinical parties due to its relevance in the areas of drug development, cell therapy, and disease modeling. While the scope of what could be achieved is wide, a number of obstacles remain before human pluripotent stem cell (hPSC) technologies can be adopted for widespread use. On the one hand are the technical challenges relating to scalability, definition, and reproducibility, while from a basic research perspective, many unanswered questions remain regarding the development of an adult phenotype, the mechanisms of cell reprogramming, and the role of the tissue culture microenvironment.

Early protocols for the generation of hepatocytes from pluripotent cells relied on the use of embryoid body formation (Baharvand et al., 2006; Basma et al., 2009; Imamura et al., 2004). This method involves the creation of cell aggregates and the spontaneous differentiation of the pluripotent population to a mixed population of cells representing the three germ layers (Itskovitz-Eldor et al., 2000). Notable improvements in efficiency and functionality have since been achieved by various groups, which based their protocols on developmental signaling and utilized adherent culture conditions. However, all directed differentiation protocols for hepatocyte-like cells (HLCs) published to date have relied on the use of recombinant growth factors such as activin A, Wnt3a, hepatocyte growth factor (HGF), oncostatin M (OSM), fibroblast growth factor 4 (FGF4), vascular endothelial growth factor (VEGF), epidermal growth factor (EGF), and bone morphogenetic protein 4 (BMP4) (Agarwal et al., 2008; Brolén et al., 2010; Cai et al., 2007; Chen et al., 2012; Hay et al., 2008; Liu et al., 2010; Si-Tayeb et al., 2010b; Song et al., 2009; Sullivan et al., 2010; Touboul et al., 2010).

Some recent progress has been made in replacing growth factors for the differentiation of mesoderm and ectoderm (Chambers et al., 2012; Lian et al., 2012), and efforts have been undertaken to find suitable candidates for the production of definitive endoderm (DE), exemplified by the Melton group, who identified IDE1 and 2 (Borowiak et al., 2009). Recent studies have also demonstrated the utility of other small molecules in priming pluripotent cells for differentiation toward endoderm (Tahamtani et al., 2013) and mesoderm (Tan et al., 2013). To date, however, further endodermal differentiation has only been performed in combination with other recombinant growth factors (for a review, see Han et al., 2012).

A number of publications have demonstrated that Wnt signaling is required to specify DE (Engert et al., 2013; Nakanishi et al., 2009), and we have found that a pulse of GSK-3 inhibition is sufficient to produce

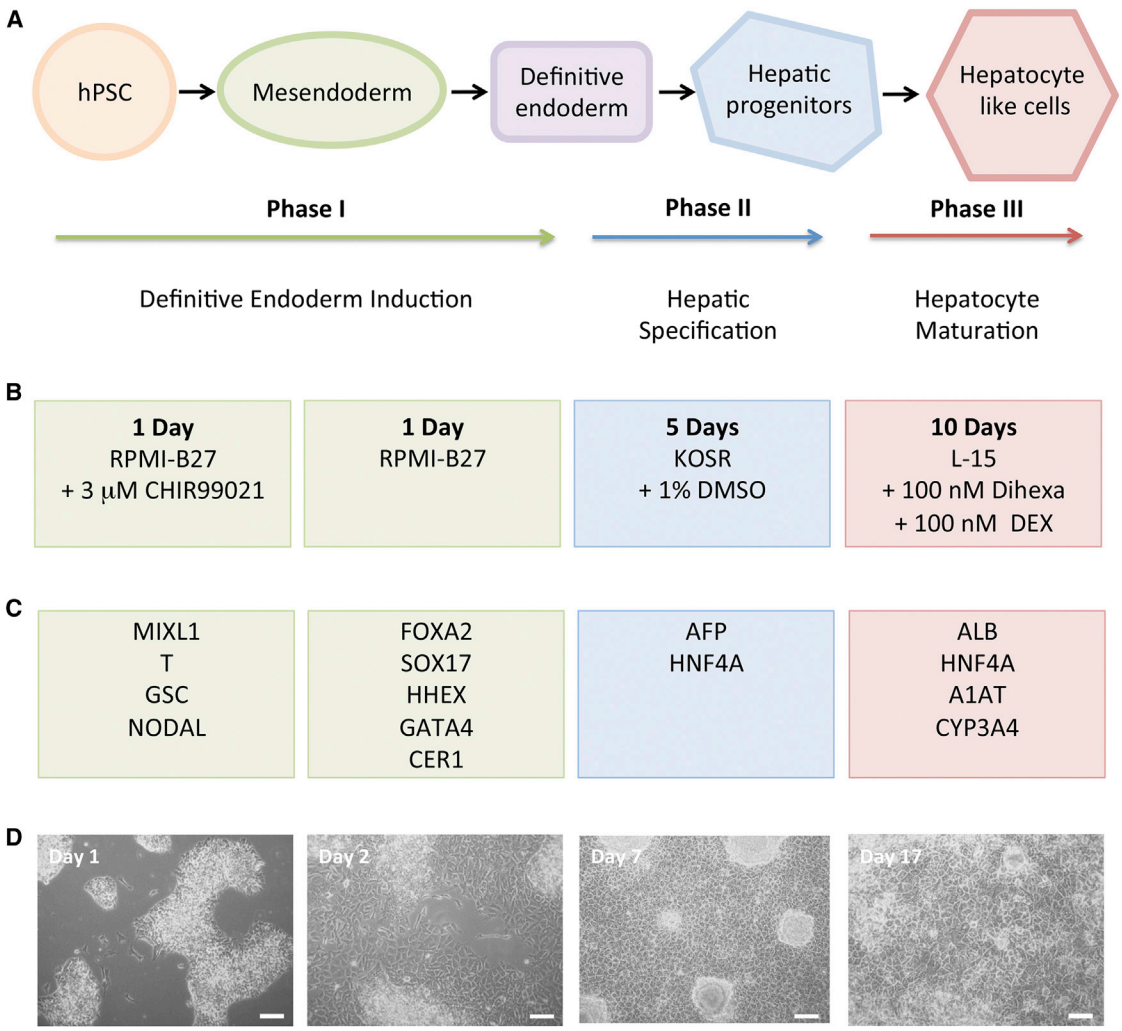


**Figure 1. Schematic of the Differentiation Process**

(A) The normal process of differentiation and the phases of the protocol to which these apply.

(B) Summary of the base media, time course, and small-molecule additions for each phase of differentiation.

(C) Key markers expressed at each stage of differentiation.

(D) Representative morphology of H1 cells observed at key stages of differentiation using phase contrast microscopy (10×). Scale bars, 100 μm.

See also Figure S1.

populations of DE at a high efficiency. We are then able to direct the small-molecule-generated population of DE to functional HLCs with a combination of small molecules, namely DMSO, dexamethasone (DEX), and an HGF receptor agonist N-hexanoic-Tyr, Ile-(6) aminohexanoic amide (dihexa) (McCoy et al., 2013). This stepwise approach is able to generate HLCs at high efficiency, without the inclusion of growth factors (Figure 1). The differentiated cells demonstrate similar levels of function to those derived via published growth-factor-based approaches.

## RESULTS

### Production of DE Using GSK-3 Inhibition: Phase I

The ability to produce hepatocytes from hPSCs that have utility in both clinical and research arenas will require methodologies that are robust in terms of efficiency and reproducibility. The majority of methodologies to date are far from this and also reliant on recombinant growth factors to direct cellular fate. This will prove a major hurdle if these cells are to be utilized in a therapeutic environment. We have therefore developed a differentiation

procedure that is devoid of growth factors and driven by small molecules. The procedure is notionally trisected into three phases inducing DE differentiation (phase I), hepatic specification (phase II), and hepatocyte maturation (phase III).

Following studies of the utility of GSK-3 inhibition in priming pluripotent cells for endodermal differentiation (Tahamtani et al., 2013) and reports that Wnt/β-catenin signaling regulates *SOX17* expression and is essential for endoderm formation (Engert et al., 2013), we set out to establish whether we could use this approach as a starting point for the generation of functional hepatocytes. We initially established the conditions for DE differentiation in the hESC line H1. Through a 24-hr treatment with 3 μM CHIR99021, followed by 24 hr of non-directed differentiation in RPMI-B27, we were able to guide hPSCs through developmentally relevant stages to produce a population of DE (Figure 2A). Over a 48-hr period, we observed dynamic changes in the gene expression pattern (Figure 3). By 48 hr, we observed elevated expression of DE markers such as *FOXA2*, *GSC*, *SOX17*, *HHEX*, and *CER1* (Ang et al., 1993; Blum et al., 1992; Kanai-Azuma et al., 2002; Monaghan et al., 1993; Sasaki and Hogan, 1993). In addition, early events of the differentiation indicated transition through a primitive streak (PS) intermediate. We observed a rapid upregulation of *NODAL* within 4 hr of exposure to CHIR99021, which is indicative of a transition toward a PS population (Figure 3) (Lu et al., 2001). This was followed by induction of the PS markers *T* and *GSC* (Figure 3). The markers *SOX17*, *GSC*, *FOXA2*, and *MIXL1* are expressed in extra-embryonic endodermal lineages as well as DE. In order to demonstrate that our differentiation procedure was not producing primitive endoderm, we examined the levels of *SOX7* and observed no upregulation during our procedure (Figure 2A). The observed patterns of expression are similar to those seen with a 3-day treatment of activin A and Wnt3a or a 5-day treatment of activin A (D'Amour et al., 2005; Hay et al., 2008). These changes in gene expression were accompanied by morphological changes; the cells shifted from a pluripotent morphology to dense, bright clusters at 24 hr, followed by a petal-like morphology at 48 hr (Figure 2B). At the 48-hr time point (phase I endpoint), we observed co-expression of FOXA2 and SOX17 at the protein level using immunofluorescence (Figure 2C). We then compared treatments with activin A/Wnt3a, CHIR99021, and vehicle control and found equivalent co-expression of the DE proteins FOXA2 and SOX17 by immunofluorescence in the growth-factor- and small-molecule-treated cells (Figure 2C) and no co-expression in the control (data not shown). Next, we assessed whether GSK-3 inhibition was a generic mechanism to drive hPSCs to DE. Figure 2C demonstrates the utility of an alternative GSK-3 inhibitor (BIO, 1 μM) to produce FOXA2/SOX17-positive cells under the same conditions, suggesting that GSK-3 inhibition followed by its removal is responsible for commitment to DE. It is well documented that BIO and CHIR99021 are potent pharmacological GSK-3-specific inhibitors that result in activation of the Wnt signaling pathway (Sato et al., 2004; Sineva and Pospelov, 2010), so we next assessed the ability of the protein Wnt3a alone to drive differentiation toward DE. Figure 2C demonstrates that treatment with Wnt3a was sufficient to produce populations of cells that expressed the DE markers FOXA2 and SOX17. This observation indicates that Wnt3a treatment alone can facilitate the production of DE and that the inclusion of activin A is not necessary for DE production in vitro. All treatments described gave similar efficiencies with respect to FOXA2- and SOX17-positive cells: 78%–85% for FOXA2 and 79%–87% for SOX17 (Figure 2D).

## Hepatic Specification through DMSO Treatment of Definitive Endoderm: Phase II

Following the production of DE through small-molecule stimulation, the next step was to specify a hepatic fate. We explored potential routes to efficiently produce an AFP/HNF4A-positive hepatic progenitor population. There are numerous reports of the utility of the small molecule DMSO in stem cell differentiation and specifically in the generation of hepatic progenitors (Hay et al., 2008; Rambhatla et al., 2003; Soto-Gutierrez et al., 2006; Sullivan et al., 2010). Therefore, we used a well-established method consisting of a 5-day treatment with 1% DMSO. On subjecting DE to phase II conditions (DMSO), we observed a rapid change in morphology and a spurt of proliferation. After the 5 days of treatment, we observed 87% co-expression of AFP and HNF4A, as assessed by immunofluorescence (Figures 4A and 4B). This was comparable to activin A/Wnt3a followed by DMSO treatment, in line with previous reports (Figures 4A and 4B). In addition, the cells exhibited typical hepatocyte progenitor morphology as assessed by phase contrast microscopy (Figure 4C). The levels of AFP/HNF4A co-expression observed are indicative that this phase of the differentiation is extremely efficient (Figure 4B). Gene expression was analyzed after the end of hepatic specification by qRT-PCR (Figure 4D), and the panel shows a repertoire of hepatic progenitor markers that were expressed including *AFP*, *CEBPA*, *FOXA2*, *GATA4*, *HNF4A*, *PROX1*, *TBX3*, and *TTR*. To assess the differentiation of DE to hepatic progenitors (hepatoblasts), we monitored the gene expression levels of several key developmental markers, which are known to regulate hepatoblast formation in vivo, during the 5-day phase II protocol (Si-Tayeb et al., 2010a). We observed that both small-molecule- and growth-factor-derived DE (hESC line H1) followed a similar trajectory toward hepatic progenitors (Figure 5). During differentiation to hepatic

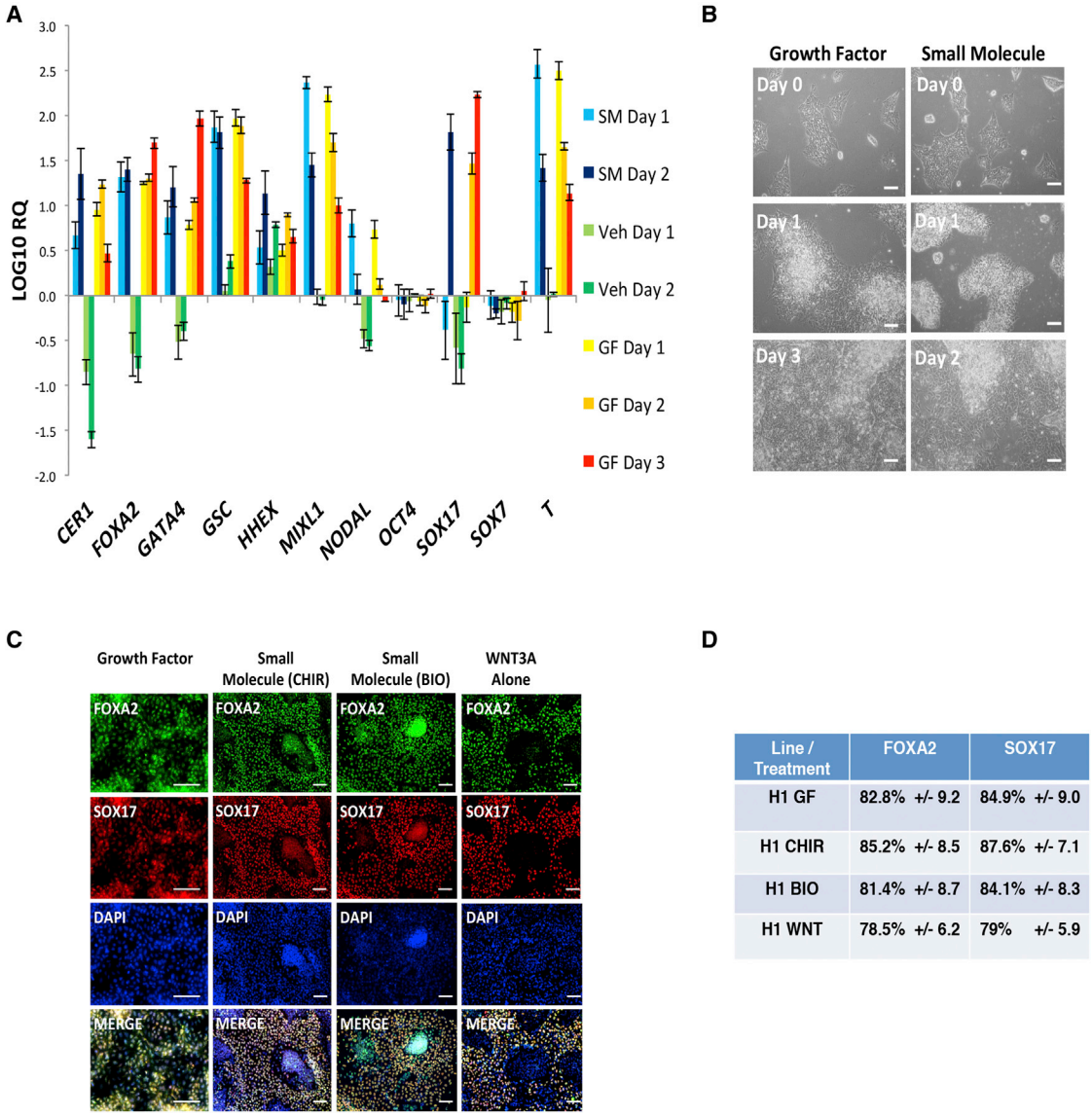


| Line / Treatment | FOXA2 | SOX17 |
|---|---|---|
| H1 GF | 82.8% +/- 9.2 | 84.9% +/- 9.0 |
| H1 CHIR | 85.2% +/- 8.5 | 87.6% +/- 7.1 |
| H1 BIO | 81.4% +/- 8.7 | 84.1% +/- 8.3 |
| H1 WNT | 78.5% +/- 6.2 | 79% +/- 5.9 |

**Figure 2. Characterization of Phase I Differentiation: Definitive Endoderm**

(A) Gene expression changes during phase I of differentiation as measured by TaqMan qRT-PCR. Blue progression, small-molecule treatment after 24 and 48 hr. Green progression, vehicle control at 24 and 48 hr. Yellow-red progression, published growth-factor-based method (Hay et al., 2008) at 24, 48, and 72 hr. All were performed using H1 hESCs and normalized to *ACTB* and undifferentiated control. Data are presented as the mean of three independent experiments; error bars represent SD.

(B) Comparison of morphology of growth factor and small-molecule definitive endoderm differentiation at days 0, 1, and 3 for growth factor and days 0, 1, and 2 for small molecule, taken using phase contrast microscopy (10×). Scale bars, 100 μm.

(C) Expression of FOXA2 and SOX17 at phase I endpoint after treatment with activin/Wnt3a, CHIR99021, BIO, or Wnt3a alone, imaged using fluorescent microscopy. The treatment is indicated at the head of each column. Scale bars, 100 μm.

(D) Efficiency of phase I differentiation, determined by counting FOXA2-positive cells and SOX17-positive cells. Efficiencies are presented as the percentage of positive cells plus or minus the SD of all fields counted.

See also Figure S2.

progenitors, we observed maintenance of *FOXA2* levels and an induction of *GATA4*, both of which are known to be pioneer factors critical to promote the hepatic gene expression program (Kaestner, 2005). Over the 5 days, there was an increase in expression of *PROX1* and *TBX3*, which are believed to interact in vivo to promote the migration and proliferation of hepatoblasts from the primary liver bud (Sosa-Pineda et al., 2000; Lüdtke et al., 2009).

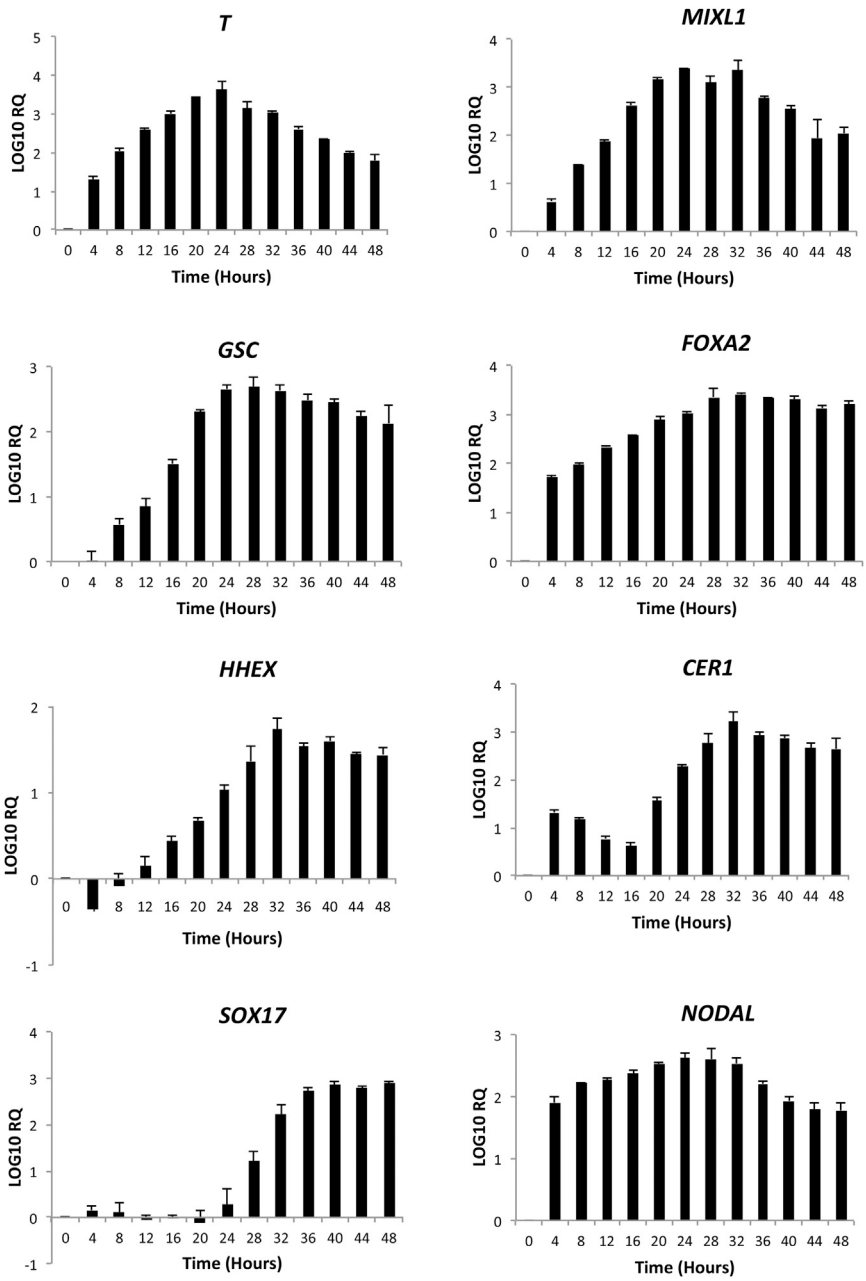


**Figure 3. Phase I 48-Hr Time Course to Assess Developmental Trajectory by qRT-PCR**

The human embryonic stem cell line H1 was differentiated in RPMI-B27 supplemented with 3 μM CHIR99021. The expression profiles of key genes were examined to establish the dynamics of the differentiation process. We monitored developmentally relevant markers of primitive streak (*T*, *MIXL1*, *GSC*, and *FOXA2*), mesendoderm (*T* and *FOXA2*), and definitive endoderm (*HHEX*, *CER1*, *SOX17*, and *FOXA2*). Cells were collected for analysis every 4 hr for 48 hr (phase I: DE stage). Data are presented as the mean of three independent experiments; error bars represent SD. The x axis represents the time (in hours) after the start of differentiation. The y axis represents the log10 relative quantification (RQ) values from the TaqMan analysis. See also Figure S3.

Furthermore, we analyzed several key regulators and markers of hepatocyte differentiation and observed strong induction of *CEBPA*, *HNF4A*, *TTR*, and *AFP*.

## Production of HLCs via Dexamethasone and the HGF Receptor Agonist Dihexa: Phase III

The final stage of HLC differentiation (hepatic maturation) has been performed by many groups using a wide range of growth factors such as HGF, OSM, FGF4, VEGF, and EGF (Han et al., 2012). We assessed the literature landscape to find potential small-molecule mimetics of growth factors involved in hepatocyte maturation and identified a potent, stable HGF receptor agonist, N-hexanoic-Tyr, Ile-(6) aminohexanoic amide (dihexa). This molecule was originally developed as a potential therapeutic intervention for neurodegenerative disorders such as Alzheimer's disease (McCoy et al., 2013). In addition, we utilized the small-molecule glucocorticoid mimetic dexamethasone (DEX), which is well established in hepatocyte maturation procedures.

We tested a number of base media to establish the optimal concentrations of DEX and dihexa. We initially

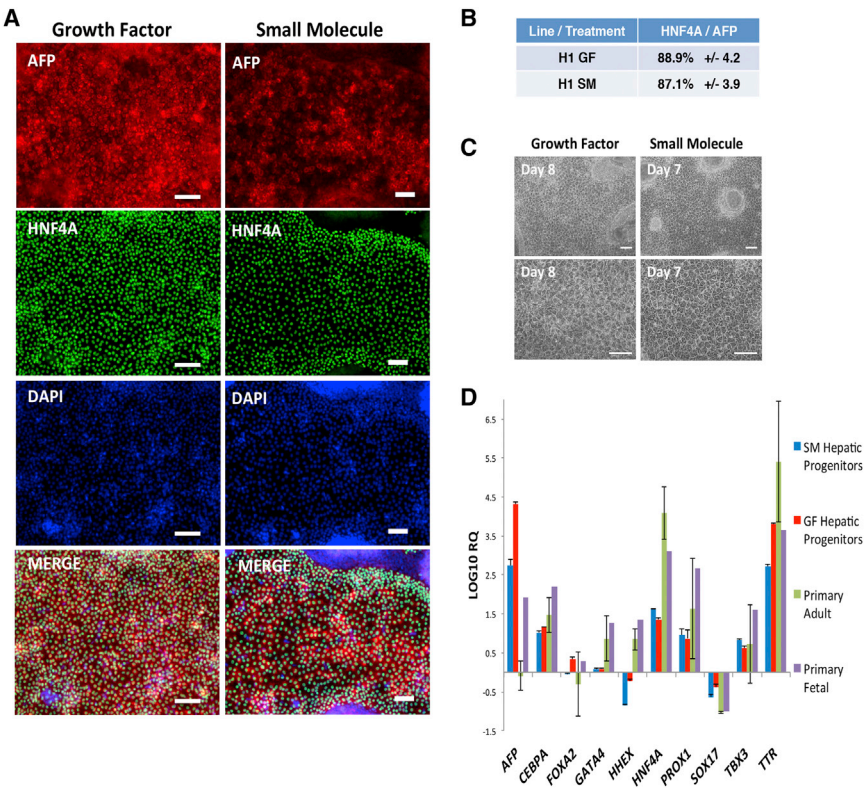


**Figure 4. Characterization of Phase II Differentiation: Hepatic Specification**

(A) Expression of AFP and HNF4A at phase II endpoint of growth-factor- and small-molecule-treated cells, imaged using fluorescent microscopy. Treatment is indicated at the head of each column. Scale bars, 100 μm.

(B) Efficiency of phase II differentiation, determined by counting AFP and HNF4A double-positive cells. Efficiencies are presented as the percentage of positive cells plus or minus the SD of all fields counted.

(C) Morphology at phase II endpoint, photographed using phase contrast microscopy at 10× and 20×. Scale bars, 100 μm.

(D) Expression of *AFP CEBPA*, *FOXA2*, *GATA4*, *HHEX*, *HNF4A*, *PROX1*, *SOX17*, *TBX3*, and *TTR* at phase II endpoint following either growth-factor (red) or small-molecule (blue) treatments, as measured by TaqMan. Normalized to *ACTB* and growth-factor- or small-molecule-derived definitive endoderm, respectively. Data are presented as the mean of three independent experiments; error bars represent SD.

See also Figure S4.

used the proprietary media HepatoZYME (Life Technologies) and established the optimal concentrations of DEX and dihexa as being 100 nM for each (data not shown). However, HepatoZYME is a proprietary reagent and contains the growth factor EGF and thus was unsuitable for this application (Garcia et al., 2001). We next assessed William's base medium, as this is used in a number of protocols for hepatocyte differentiation. Both DEX and dihexa were required, and the above concentrations gave the best results in terms of morphology and function, but this media was not optimal in our hands (data not shown). We finally settled on a modified formulation of Leibovitz L-15 medium (L-15), which has been described in the literature as a standard method to generate mature hepatocytes (Hay et al., 2008; Sullivan et al., 2010). L-15 medium was supplemented with DEX and dihexa (both at 100 nM), which led to the production of cells displaying typical hepatocyte morphology at the endpoint of the small-molecule-driven differentiation protocol (Figure 6A). The cells were large and angular with bright junctions and in some instances contained multiple nuclei. The resulting HLCs demonstrated expression of the hepatocyte markers albumin (ALB), HNF4A, alpha-1-antitrypsin (A1AT), and AFP by immunofluorescence (Figures 6B–6D). Comparable data can be seen for growth-factor-based differentiation in Figures 6B–6D. We observed comparable efficiencies of differentiation between the growth-factor and small-molecule approaches by assessing ALB/HNF4A, A1AT, and AFP (Figure 6E). To corroborate that the source of the HLCs is from DE rather than from yolk sac, we demonstrated that the DE origin marker *CYP7A1* was expressed (Asahina et al., 2004) (Figure 6F). To ensure that the protocol was equivalent to previously described growth-factor-based methods, we produced functional hepatocytes as described by Hay and colleagues (Hay et al., 2008) (see Figures 6B–6D) for validation. Gene expression was analyzed by qRT-PCR (Figure 7A), and the panel shows a repertoire of hepatic markers that were expressed: *A1AT (SERPINA1)*, *AFP*, *ALB*, *APOA2*, *ASGR1*, *CYP3A4*, *HNF4A*, *TDO2*, and *TTR*. The observed relative levels of expression were very similar irrespective of being derived via the growth-factor- or small-molecule-based protocol (Figure 7A). We observed similar level of expression with respect to fetal hepatocytes for *A1AT (SERPINA1)*, *APOA2*, *ASGR1*, *HNF4A*, and *TTR*. However, we observed higher levels of expression of *AFP* for both small-molecule- and growth-factor-derived HLCs compared to adult and fetal hepatocytes. In all cases, except for *AFP*, we observed higher levels of expression of all hepatic markers in primary adult hepatocytes.

## Small-Molecule-Derived HLCs Demonstrate Hepatic Function

Above, we have shown that small-molecule-derived HLCs (smHLCs) exhibit hepatic morphology and expression of

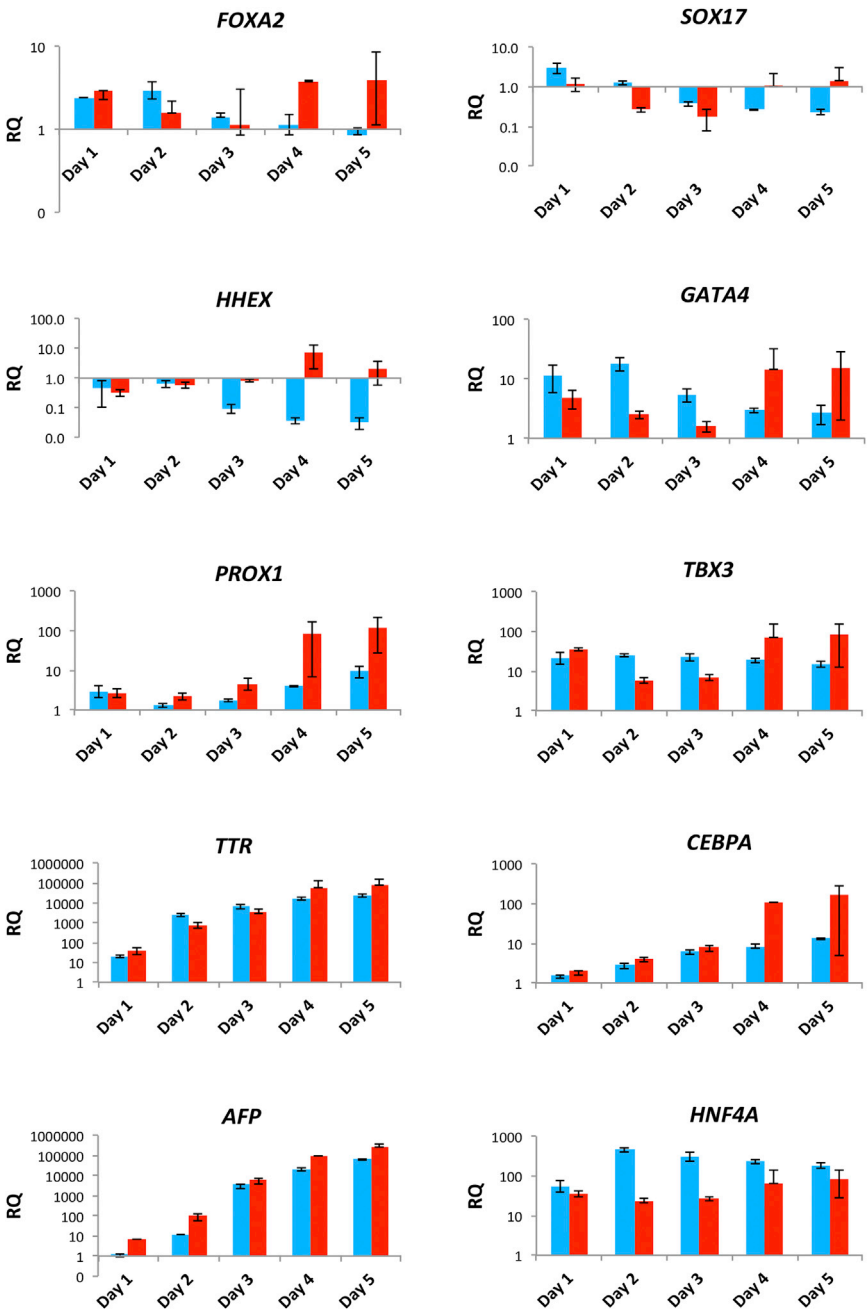


**Figure 5. Phase II 5-Day Time Course**

The human embryonic stem cell line H1 was differentiated to definitive endoderm using either the small-molecule (blue) or growth-factor (red) protocol. Definitive endoderm was treated with 1% DMSO to differentiate to hepatic progenitors, and cells were collected every 24 hr for 5 days to assess the gene expression of developmentally relevant hepatic markers. Data are presented as the mean of three independent experiments; error bars represent SD. The x axis represents the time (in days) after definitive endoderm. The y axis represents the RQ values from the TaqMan analysis. See also Figure S5.

hepatocyte-specific markers at the transcriptional and protein levels. We next assessed whether smHLCs displayed functional hepatic characteristics. An important function of hepatocytes is the ability to clear xenobiotics via metabolism through the cytochrome P450 isoenzymes. We assessed smHLCs for their metabolic potential, as compared to growth-factor-derived HLCs. The cytochrome P450 enzymes (CYP) are critical in drug metabolism, in particular CYP1A2 and CYP3A4. We assessed the function of these CYPs in terms of their basal activity and their ability to be induced by rifampicin (CYP3A4) and omeprazole (CYP1A2). We observed higher basal CYP activity in the smHLCs as compared to hESC H1 controls for both CYP1A2 and 3A4 (Figure 7B). On challenge with known inducers of these enzymes, we observed significant induction of both CYPs, to a similar degree as in growth-factor-derived HLCs (Figure 7B). Another key function of hepatocytes is the production of serum proteins, so we examined the ability of the smHLCs to secrete albumin, alpha-1-antitrypsin, and fibronectin by ELISA. All three proteins were

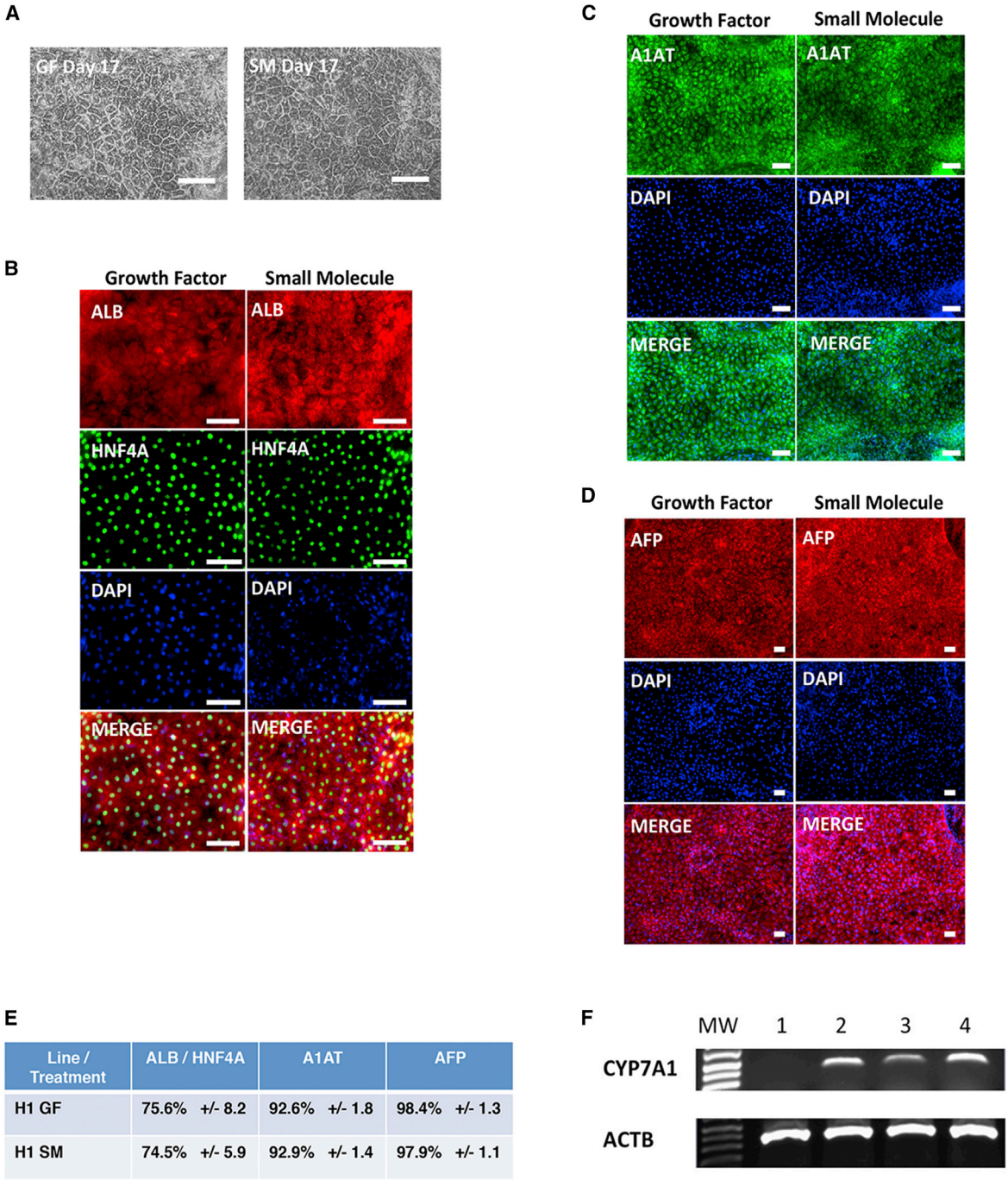


E

| Line / Treatment | ALB / HNF4A | A1AT | AFP |
|---|---|---|---|
| H1 GF | 75.6% +/- 8.2 | 92.6% +/- 1.8 | 98.4% +/- 1.3 |
| H1 SM | 74.5% +/- 5.9 | 92.9% +/- 1.4 | 97.9% +/- 1.1 |




**Figure 6. Characterization of Phase III Differentiation to Hepatocyte-like Cells: Morphology and Immunofluorescence**

(A) Morphology of growth-factor and small-molecule protocol endpoints, taken using phase contrast microscopy at 10×. Scale bars, 100 μm.

(B) Expression of albumin and HNF4A at protocol endpoints, imaged using fluorescent microscopy. Treatment is indicated at the head of each column. Scale bars, 100 μm.

(C) Expression of A1AT at protocol endpoints, imaged using fluorescent microscopy. Treatment is indicated at the head of each column. Scale bars, 100 μm.

(D) Expression of AFP at protocol endpoint was imaged using fluorescent microscopy. Treatment is indicated at the head of each column. Scale bars, 100 μm.

*(legend continued on next page)*

detected in the medium at levels similar to those seen from growth-factor-derived cells (Figure 7C). Another function tested was the ability to store glycogen. smHLCs were stained with periodic acid Schiff (PAS) and counter-stained with H&E. We observed extensive cytoplasmic staining (pink to purple), indicative of glycogen storage, at levels similar to those observed in growth-factor-derived hepatocytes (Figure 7D). We also examined the uptake of indocyanine green (ICG) in smHLCs; after a brief treatment, ICG-positive cells were clearly visible (Figure 7E).

### smHLCs Can Be Derived from Multiple Human Pluripotent Stem Cell Lines

An important attribute of any differentiation methodology is the ability to translate it to other cell lines. This is especially important in the case of hiPSCs, as these will provide a basis to model hepatic disease and potentially lead to the development of personalized medicine. In addition, the ability to derive hepatocytes of a defined genotype will be of utility in the areas of toxicology and drug development. To test this, we assessed the potential of a number of hPSC lines. We tested one additional hESC line (207) and three different hiPSC clones derived from the fibroblast line Detroit 551 (RA, RB, and RC), using the conditions applied to the hESC line H1.

Through an initial 24-hr treatment with 3 μM CHIR99021, followed by 24 hr of non-directed differentiation in RPMI-B27, we observed that the differentiation was very inefficient and did not produce the predicted morphology (data not shown) as previously observed for the hESC line H1 (Figure 2B). We next performed a titration of the small molecule CHIR99021 (1–10 μM) in RPMI-B27 ± insulin (Figure S1C). The optimal concentration for CHIR99021 was 4 μM in RPMI-B27 minus insulin in all cases. Over a 48-hr period, we observed dynamic changes in the gene expression pattern (Figure S2A) similar to those previously observed for the hESC line H1. On completion of phase I (48 hr), we observed elevated expression of DE markers such as *FOXA2*, *GSC*, *SOX17*, *HHEX*, and *CER1*. These changes in gene expression were accompanied by morphological changes consistent with the hESC line H1 differentiation above (Figure S2B). At the 48-hr time point (phase I endpoint), we observed co-expression of FOXA2 and SOX17 at the protein level using immunofluorescence (Figure S2C). All lines gave similar efficiencies with respect to FOXA2- and SOX17-positive cells: 81%–84% for FOXA2 and 79%–82% for SOX17 (Figure S2D). To ensure that hiPSCs were following a developmentally relevant route, we assessed the timing of key events in DE specification. Figure S3 shows induction of the PS markers *T*, *GSC*, and *NODAL* in the first 24 hr. This is followed by specification to definitive endoderm indicated by robust induction of *SOX17*, *GSC*, *FOXA2*, and *MIXL1* (Figure S3) and no significant upregulation of *SOX7* (Figure S2A).

On confirmation of DE specification, we next sought to specify a hepatic fate. We utilized the same phase II conditions (DMSO) as described above. After the 5 days of treatment, we observed a rapid change in morphology, accompanied with proliferation. For all lines tested, we observed typical hepatic progenitor morphology as assessed by phase contrast microscopy (Figure S4A). We observed efficiencies of between 86% and 89% based on AFP/HNF4A co-expression, as assessed by immunofluorescence (Figures S4B and S4C). Gene expression was analyzed after the end of hepatic specification by qRT-PCR, at which point we observed equivalent expression profiles as hESC H1 (Figure S4D). In addition, as with the hESC line H1, we performed a time course over 5 days and observed a very similar developmental marker profile (Figure S5). The validated hepatic progenitor cells from the different hPSCs were then subjected to phase III differentiation (Figures 1C and S1C). On completion of the differentiation, all lines efficiently generated smHLCs as assessed by morphology (Figure S6A). All lines demonstrated extensive expression of ALB/ HNF4A and alpha-1-antitrypsin by immunofluorescence (Figures S6B and S6C). Both hESC line 207 and hiPSC-derived smHLCs secreted albumin, alpha-1-antitrypsin, and fibronectin as assessed by ELISA. All three proteins were detected in the medium at levels similar to those observed for H1 (Figures S7A). We demonstrated that the hiPSC-derived smHLCs were from a DE origin via the presence of *CYP7A1* (Figure S7B). We observed comparable efficiency of smHLC production to hESC H1 (between 72% and 79% for ALB/HNF4A and between 88% and 92% for A1AT; Figure S7C). Finally we assessed the expression levels of the following hepatocyte markers: *A1AT (SERPINA1)*, *AFP*, *ALB*, *APOA2*, *ASGR1*, *CYP3A4*, *HNF4A*, *TDO2*, and *TTR* by qRT-PCR, and profiles very similar to H1-derived smHLCs were observed (Figure S7C). Thus, we demonstrated that our protocol was applicable to other hESC and hiPSC lines.

(E) Efficiency of phase III differentiation, determined by counting albumin and HNF4A double-positive cells, A1AT-positive cells, and AFP-positive cells. Efficiencies are presented as the percentage of positive cells plus or minus the SD of all fields counted.
(F) RT-PCR of *CYP7A1* gene expression of H1-derived smHLCs. Lane 1, hESC H1 control; lanes 2–4 (top panel), H1 day 17 HLCs *CYP7A1* expression; lanes 2–4 (lower panel), *ACTB* loading control.
See also Figure S6.

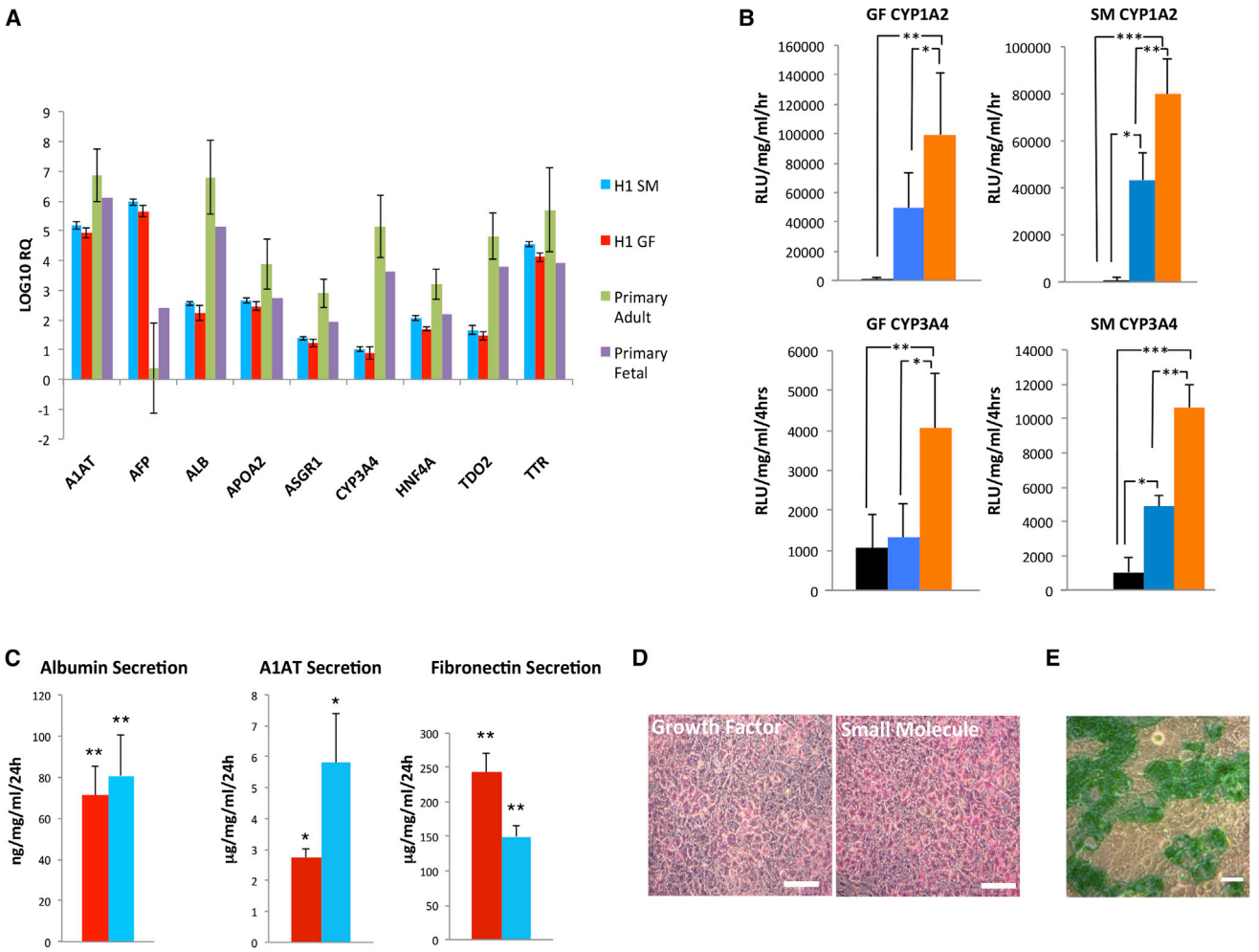


**Figure 7. Characterization of Phase III Differentiation to Hepatocyte-like Cells: qRT-PCR and Functional Analysis**

(A) Expression of *A1AT (SERPINA1)*, *AFP*, *ALB*, *APOA2*, *ASGR1*, *CYP3A4*, *HNF4A*, *TDO2*, and *TTR* at endpoint of small-molecule (blue) and growth-factor (red) protocols, as well as primary adult and fetal hepatocyte controls, assessed by TaqMan. Normalized to *ACTB* and small-molecule- or growth-factor-derived definitive endoderm, respectively. Data are presented as the mean of three independent experiments; error bars represent SD. Because only one primary fetal control was run, no error bars are present.

(B) Cytochrome P450 1A2 and 3A4 activity and induction were assessed in both smHLCs (SM) and growth-factor-derived HLCs (GF). The black columns represent hESC H1 pluripotent control, the blue columns represent basal activity, and the orange columns represent activity after induction with either omeprazole (1A2) or rifampicin (3A4). Data are presented as the mean of six independent experiments; error bars represent SD (n = 6 biological replicates). GF CYP1A2 *$p < 0.05$, **$p < 0.002$; SM CYP1A2 *$p < 0.02$, **$p < 0.01$; ***$p < 0.001$. GF CYP3A4 *$p < 0.001$, **$p < 0.005$; SM CYP3A4 *$p < 0.004$, **$p < 0.0002$; ***$p < 2 \times 10^{-5}$.

(C) Serum protein secretion at endpoint of both growth-factor- (red) and small-molecule-based (blue) protocols. Data are presented as the mean of three independent experiments; error bars represent SD. *$p < 0.09$, **$p < 0.004$, compared to control.

(D) Glycogen storage in growth-factor- and small-molecule-differentiated cells as indicated by PAS staining. Treatment is indicated top left of each panel. Scale bars, 100 µm.

(E) H1 smHLCs treated for 1 hr with 1 mg/ml indocyanine green demonstrate uptake as assessed by phase microscopy. Scale bars, 100 µm. See also Figure S7.

## DISCUSSION

We have developed a protocol for the efficient differentiation of functional HLCs from hPSCs that does not require the addition of recombinant growth factors and is applicable to both hESCs and hiPSCs. During the development of the protocol, it came as a surprise to discover that pluripotent cells can be differentiated to DE with a short pulse (24 hr) of CHIR99021, BIO, or Wnt3a without the inclusion of activin A. The rationale to examine GSK-3

inhibition as a route to producing DE has a basis in the observations of Lickert and colleagues (Engert et al., 2013), who demonstrated that Wnt signaling regulates SOX17 expression. A number of other publications also describe the priming activity of GSK-3 inhibitors such as CHIR99021 (Hannan et al., 2013; Kunisada et al., 2012; Tahamtani et al., 2013; Tan et al., 2013). In this study, we clearly demonstrate that GSK-3 inhibition alone is sufficient to produce DE, a finding that in itself represents an opportunity for major saving in hepatocyte-production costs. Importantly, this first stage provided productive DE, which expressed a battery of DE markers including SOX17 and FOXA2, and passed through the equivalent developmental points as growth factor DE (Figure 2A). The use of DMSO to drive DE toward a hepatic fate is well established in the field (Hay et al., 2008; Soto-Gutiérrez et al., 2007; Sullivan et al., 2010), and we show here that it is equally successful when employed following CHIR99021 treatment as with activin A and Wnt3a. We observed a rapid change in morphology, coupled with the appearance of the hepatic progenitor markers HNF4A and AFP, both at the transcriptional and protein levels. The final phase of this protocol was to take hepatic progenitors and provide the environment for hepatocyte maturation in order to generate HLCs. We chose to utilize a combination of two small molecules of the glucocorticoid family, DEX and hydrocortisone-21-hemisuccinate (HC), and assessed the literature for potential mimetics of commonly used growth factors. We identified a potent HGF mimetic called N-hexanoic-Tyr, Ile-(6) aminohexanoic amide, or dihexa, originally developed as an anti-dementia drug (McCoy et al., 2013). This molecule was identified in a screen that assessed the capacity to potentiate the biological activity of HGF. We therefore employed the small molecules DEX, HC and dihexa in phase III of the protocol. Initially, phase III was optimized using the commercially available base medium HepatoZYME that has been shown to provide supportive conditions for hepatocyte maturation (Szkolnicka et al., 2014). We demonstrated the dependency of dihexa in this system (data not shown), but it transpired that HepatoZYME is not growth factor free and contains the morphogen EGF (Garcia et al., 2001). We then translated our findings to the routinely used hepatocyte maturation medium L-15, which others have used supplemented with a combination of growth factors and small molecules (Hay et al., 2008; Sullivan et al., 2010). We supplemented L-15 with the aforementioned small molecules and efficiently generated HLCs from both hESCs and hiPSCs, which displayed typical hepatic morphology and expressed a number of hepatic markers at the transcriptional and protein levels. More importantly, the smHLCs exhibited key functional attributes including serum protein production and cytochrome P450 metabolism. It should be stated that we used the P450-Glo assay system (Promega) to initially assess function with respect to CYP activity as in line with many other publications. But, in order to gain a thorough insight into the metabolic potential of these cells, we will need to assess them using the more robust and accepted methods including mass spectrometry and high-performance liquid chromatography. It should be noted that the above method is not fully defined at this point, as the present L-15 formulation contains 8.3% serum. We are currently investigating avenues to generate a completely defined system for the production of hepatocytes, but the method described here represents a significant step toward this goal and is applicable to both hESC and hiPSC lines. Importantly, it provides a means to cut the costs associated with hepatocyte production. A combination of this small-molecule approach with the steadily advancing field of cell-culture automation may eventually allow for the production of high-quality hepatocytes from stem cells at large scale for industrial and clinical translation. In the meantime, this approach in our hands produces cells of equivalent phenotype and function to current approaches and addresses some of the cost, quality, and supply-chain concerns associated with reliance on recombinant growth factors.

In conclusion, we demonstrate here the efficient generation of both hESC- and hiPSC-derived HLCs through the use of small molecules, removing the longstanding reliance on recombinant growth factors. This may go on to provide the foundations for scalable hepatocyte production for use in disease modeling, cell therapy, drug discovery, and basic research in terms of improving maturity and function in vitro.

## EXPERIMENTAL PROCEDURES

### Cell Culture

H1 hESCs (WiCell) and 207 hESCs (Ström et al., 2010) and Detroit 551 (ATCC CCL-110) hiPSCs were maintained at 37°C/5% $CO_2$ in feeder-free conditions using growth-factor-reduced Matrigel (Sigma-Aldrich) and E8 Medium (Life Technologies), with routine passaging performed at a 1:3 ratio using 0.5 mM EDTA (Life Technologies). All Matrigel plates were coated with a 1:48 dilution in Advanced DMEM-F12 (Life Technologies) and incubated at 37°C/5% $CO_2$ for 1 hr prior to use.

### Hepatocyte Differentiation

Cells were seeded onto Matrigel-coated 12-well plates in E8 medium at a 1:3–1:4 split ratio and allowed to adhere for 24 hr at 37°C/5% $CO_2$. It should be noted that the optimal cell density for each line needs to be established. The cells were washed with PBS before being treated with differentiation media. The differentiation protocol utilizes a base media similar to a well-established differentiation protocol (Hay et al., 2008), with replacement of

all growth factors with small molecules and minor adjustments in timing. The protocol incorporates several stages (Figure 1) utilizing different small molecules.

Phase I of differentiation consists of a 24-hr treatment with RPMI-B27 ± insulin (RPMI 1640 GlutaMAX + B27 supplement, both from Life Technologies) plus 3–4 μM CHIR99021 (Stemgent), followed by a 24-hr treatment with RPMI-B27 alone. Phase II consists of 5 days of treatment with knockout DMEM containing 20% knockout serum replacement, 2 mM GlutaMAX, 100 μM 2-mercaptoethanol, 1× MEM non-essential amino acids (Life Technologies), and 1% DMSO (Sigma-Aldrich). Phase III consists of 10 days of treatment with Leibovitz L-15 media containing 8.3% tryptose phosphate broth, 10 μM hydrocortisone 21-hemisuccinate, 50 μg/ml sodium-L-ascorbate, 100 nM dexamethasone (all from Sigma-Aldrich), 0.58% insulin-transferrin-selenium (ITS), 2 mM GlutaMAX (all from Life Technologies), 8.3% fetal bovine serum (Lonza), and 100 nM dihexa (a kind gift from Prof. Joseph Harding, Washington State University). During phases II and III, cells are fed every 48 hr. Cells were photographed during differentiation using a Zeiss phase contrast microscope and ZEN software. The scale bars represent 100 μm.

Control H1 hESCs (growth factor) were differentiated using activin A, Wnt3a, DMSO, OSM, and HGF (Peprotech) as described previously (Hay et al., 2008; Sullivan et al., 2010). All small molecules were made up in DMSO; vehicle control differentiations were performed using equivalent concentrations.

### Small Molecules

For a complete list of small molecules, sources, and purity, please see Table S4.

Detailed methods are described in the Supplemental Experimental Procedures.

## SUPPLEMENTAL INFORMATION

Supplemental Information includes Supplemental Experimental Procedures, seven figures, and four tables and can be found with this article online at http://dx.doi.org/10.1016/j.stemcr.2015.04.001.

## AUTHOR CONTRIBUTIONS

S.G. and R.S. contributed equally to this work. S.G., R.S., and G.J.S. were all extensively involved in designing, performing, and analyzing the experiments. E.N. was involved in data acquisition and analysis. S.G., R.S., and G.J.S. wrote and revised the paper.

## ACKNOWLEDGMENTS

We would like to thank Prof. Joseph Harding for the gift of dihexa. This paper will form the basis of a patent application on which S.G. and G.J.S. are named as inventors.

Received: April 16, 2014
Revised: April 2, 2015
Accepted: April 2, 2015
Published: April 30, 2015

## REFERENCES

Agarwal, S., Holton, K.L., and Lanza, R. (2008). Efficient differentiation of functional hepatocytes from human embryonic stem cells. Stem Cells *26*, 1117–1127.

Ang, S.L., Wierda, A., Wong, D., Stevens, K.A., Cascio, S., Rossant, J., and Zaret, K.S. (1993). The formation and maintenance of the definitive endoderm lineage in the mouse: involvement of HNF3/forkhead proteins. Development *119*, 1301–1315.

Asahina, K., Fujimori, H., Shimizu-Saito, K., Kumashiro, Y., Okamura, K., Tanaka, Y., Teramoto, K., Arii, S., and Teraoka, H. (2004). Expression of the liver-specific gene Cyp7a1 reveals hepatic differentiation in embryoid bodies derived from mouse embryonic stem cells. Genes Cells *9*, 1297–1308.

Baharvand, H., Hashemi, S.M., Kazemi Ashtiani, S., and Farrokhi, A. (2006). Differentiation of human embryonic stem cells into hepatocytes in 2D and 3D culture systems in vitro. Int. J. Dev. Biol. *50*, 645–652.

Basma, H., Soto-Gutiérrez, A., Yannam, G.R., Liu, L., Ito, R., Yamamoto, T., Ellis, E., Carson, S.D., Sato, S., Chen, Y., et al. (2009). Differentiation and transplantation of human embryonic stem cell-derived hepatocytes. Gastroenterology *136*, 990–999.

Blum, M., Gaunt, S.J., Cho, K.W., Steinbeisser, H., Blumberg, B., Bittner, D., and De Robertis, E.M. (1992). Gastrulation in the mouse: the role of the homeobox gene goosecoid. Cell *69*, 1097–1106.

Borowiak, M., Maehr, R., Chen, S., Chen, A.E., Tang, W., Fox, J.L., Schreiber, S.L., and Melton, D.A. (2009). Small molecules efficiently direct endodermal differentiation of mouse and human embryonic stem cells. Cell Stem Cell *4*, 348–358.

Brolén, G., Sivertsson, L., Björquist, P., Eriksson, G., Ek, M., Semb, H., Johansson, I., Andersson, T.B., Ingelman-Sundberg, M., and Heins, N. (2010). Hepatocyte-like cells derived from human embryonic stem cells specifically via definitive endoderm and a progenitor stage. J. Biotechnol. *145*, 284–294.

Cai, J., Zhao, Y., Liu, Y., Ye, F., Song, Z., Qin, H., Meng, S., Chen, Y., Zhou, R., Song, X., et al. (2007). Directed differentiation of human embryonic stem cells into functional hepatic cells. Hepatology *45*, 1229–1239.

Chambers, S.M., Qi, Y., Mica, Y., Lee, G., Zhang, X.-J., Niu, L., Bilsland, J., Cao, L., Stevens, E., Whiting, P., et al. (2012). Combined small-molecule inhibition accelerates developmental timing and converts human pluripotent stem cells into nociceptors. Nat. Biotechnol. *30*, 715–720.

Chen, Y.-F., Tseng, C.-Y., Wang, H.-W., Kuo, H.-C., Yang, V.W., and Lee, O.K. (2012). Rapid generation of mature hepatocyte-like cells from human induced pluripotent stem cells by an efficient three-step protocol. Hepatology *55*, 1193–1203.

D'Amour, K.A., Agulnick, A.D., Eliazer, S., Kelly, O.G., Kroon, E., and Baetge, E.E. (2005). Efficient differentiation of human embryonic stem cells to definitive endoderm. Nat. Biotechnol. *23*, 1534–1541.

Engert, S., Burtscher, I., Liao, W.P., Dulev, S., Schotta, G., and Lickert, H. (2013). Wnt/β-catenin signalling regulates Sox17 expression and is essential for organizer and endoderm formation in the mouse. Development *140*, 3128–3138.

Garcia, M.C., Thangavel, C., and Shapiro, B.H. (2001). Epidermal growth factor regulation of female-dependent CYP2A1 and CYP2C12 in primary rat hepatocyte culture. Drug Metab. Dispos. *29*, 111–120.

Han, S., Bourdon, A., Hamou, W., Dziedzic, N., Goldman, O., and Gouon-Evans, V. (2012). Generation of functional hepatic cells from pluripotent stem cells. J. Stem Cell Res. Ther. (*Suppl 10*), 1–7.

Hannan, N.R.F., Segeritz, C.-P., Touboul, T., and Vallier, L. (2013). Production of hepatocyte-like cells from human pluripotent stem cells. Nat. Protoc. *8*, 430–437.

Hay, D.C., Fletcher, J., Payne, C., Terrace, J.D., Gallagher, R.C.J., Snoeys, J., Black, J.R., Wojtacha, D., Samuel, K., Hannoun, Z., et al. (2008). Highly efficient differentiation of hESCs to functional hepatic endoderm requires ActivinA and Wnt3a signaling. Proc. Natl. Acad. Sci. USA *105*, 12301–12306.

Imamura, T., Cui, L., Teng, R., Johkura, K., Okouchi, Y., Asanuma, K., Ogiwara, N., and Sasaki, K. (2004). Embryonic stem cell-derived embryoid bodies in three-dimensional culture system form hepatocyte-like cells in vitro and in vivo. Tissue Eng. *10*, 1716–1724.

Itskovitz-Eldor, J., Schuldiner, M., Karsenti, D., Eden, A., Yanuka, O., Amit, M., Soreq, H., and Benvenisty, N. (2000). Differentiation of human embryonic stem cells into embryoid bodies compromising the three embryonic germ layers. Mol. Med. *6*, 88–95.

Kaestner, K.H. (2005). The making of the liver: developmental competence in foregut endoderm and induction of the hepatogenic program. Cell Cycle *4*, 1146–1148.

Kanai-Azuma, M., Kanai, Y., Gad, J.M., Tajima, Y., Taya, C., Kurohmaru, M., Sanai, Y., Yonekawa, H., Yazaki, K., Tam, P.P.L., and Hayashi, Y. (2002). Depletion of definitive gut endoderm in Sox17-null mutant mice. Development *129*, 2367–2379.

Kunisada, Y., Tsubooka-Yamazoe, N., Shoji, M., and Hosoya, M. (2012). Small molecules induce efficient differentiation into insulin-producing cells from human induced pluripotent stem cells. Stem Cell Res. (Amst.) *8*, 274–284.

Lian, X., Hsiao, C., Wilson, G., Zhu, K., Hazeltine, L.B., Azarin, S.M., Raval, K.K., Zhang, J., Kamp, T.J., and Palecek, S.P. (2012). Robust cardiomyocyte differentiation from human pluripotent stem cells via temporal modulation of canonical Wnt signaling. Proc. Natl. Acad. Sci. USA *109*, E1848–E1857.

Liu, H., Ye, Z., Kim, Y., Sharkis, S., and Jang, Y.-Y. (2010). Generation of endoderm-derived human induced pluripotent stem cells from primary hepatocytes. Hepatology *51*, 1810–1819.

Lu, C.C., Brennan, J., and Robertson, E.J. (2001). From fertilization to gastrulation: axis formation in the mouse embryo. Curr. Opin. Genet. Dev. *11*, 384–392.

Lüdtke, T.H.-W., Christoffels, V.M., Petry, M., and Kispert, A. (2009). Tbx3 promotes liver bud expansion during mouse development by suppression of cholangiocyte differentiation. Hepatology *49*, 969–978.

McCoy, A.T., Benoist, C.C., Wright, J.W., Kawas, L.H., Bule-Ghogare, J.M., Zhu, M., Appleyard, S.M., Wayman, G.A., and Harding, J.W. (2013). Evaluation of metabolically stabilized angiotensin IV analogs as procognitive/antidementia agents. J. Pharmacol. Exp. Ther. *344*, 141–154.

Monaghan, A.P., Kaestner, K.H., Grau, E., and Schütz, G. (1993). Postimplantation expression patterns indicate a role for the mouse forkhead/HNF-3 alpha, beta and gamma genes in determination of the definitive endoderm, chordamesoderm and neuroectoderm. Development *119*, 567–578.

Nakanishi, M., Kurisaki, A., Hayashi, Y., Warashina, M., Ishiura, S., Kusuda-Furue, M., and Asashima, M. (2009). Directed induction of anterior and posterior primitive streak by Wnt from embryonic stem cells cultured in a chemically defined serum-free medium. FASEB J. *23*, 114–122.

Rambhatla, L., Chiu, C.-P., Kundu, P., Peng, Y., and Carpenter, M.K. (2003). Generation of hepatocyte-like cells from human embryonic stem cells. Cell Transplant. *12*, 1–11.

Sasaki, H., and Hogan, B.L. (1993). Differential expression of multiple fork head related genes during gastrulation and axial pattern formation in the mouse embryo. Development *118*, 47–59.

Sato, N., Meijer, L., Skaltsounis, L., Greengard, P., and Brivanlou, A.H. (2004). Maintenance of pluripotency in human and mouse embryonic stem cells through activation of Wnt signaling by a pharmacological GSK-3-specific inhibitor. Nat. Med. *10*, 55–63.

Schwartz, S.D., Hubschman, J.-P., Heilwell, G., Franco-Cardenas, V., Pan, C.K., Ostrick, R.M., Mickunas, E., Gay, R., Klimanskaya, I., and Lanza, R. (2012). Embryonic stem cell trials for macular degeneration: a preliminary report. Lancet *379*, 713–720.

Si-Tayeb, K., Lemaigre, F.P., and Duncan, S.A. (2010a). Organogenesis and development of the liver. Dev. Cell *18*, 175–189.

Si-Tayeb, K., Noto, F.K., Nagaoka, M., Li, J., Battle, M.A., Duris, C., North, P.E., Dalton, S., and Duncan, S.A. (2010b). Highly efficient generation of human hepatocyte-like cells from induced pluripotent stem cells. Hepatology *51*, 297–305.

Sineva, G.S., and Pospelov, V.A. (2010). Inhibition of GSK3beta enhances both adhesive and signalling activities of beta-catenin in mouse embryonic stem cells. Biol. Cell *102*, 549–560.

Song, Z., Cai, J., Liu, Y., Zhao, D., Yong, J., Duo, S., Song, X., Guo, Y., Zhao, Y., Qin, H., et al. (2009). Efficient generation of hepatocyte-like cells from human induced pluripotent stem cells. Cell Res. *19*, 1233–1242.

Sosa-Pineda, B., Wigle, J.T., and Oliver, G. (2000). Hepatocyte migration during liver development requires Prox1. Nat. Genet. *25*, 254–255.

Soto-Gutierrez, A., Navarro-Alvarez, N., Rivas-Carrillo, J.D., Chen, Y., Yamatsuji, T., Tanaka, N., and Kobayashi, N. (2006). Differentiation of human embryonic stem cells to hepatocytes using deleted variant of HGF and poly-amino-urethane-coated nonwoven polytetrafluoroethylene fabric. Cell Transplant. *15*, 335–341.

Soto-Gutiérrez, A., Navarro-Alvarez, N., Zhao, D., Rivas-Carrillo, J.D., Lebkowski, J., Tanaka, N., Fox, I.J., and Kobayashi, N. (2007). Differentiation of mouse embryonic stem cells to hepatocyte-like cells by co-culture with human liver nonparenchymal cell lines. Nat. Protoc. *2*, 347–356.

Ström, S., Holm, F., Bergström, R., Strömberg, A.-M., and Hovatta, O. (2010). Derivation of 30 human embryonic stem cell lines—improving the quality. In Vitro Cell. Dev. Biol. Anim. *46*, 337–344.

Sullivan, G.J., Hay, D.C., Park, I.-H., Fletcher, J., Hannoun, Z., Payne, C.M., Dalgetty, D., Black, J.R., Ross, J.A., Samuel, K., et al. (2010). Generation of functional human hepatic endoderm from human induced pluripotent stem cells. Hepatology *51*, 329–335.

Szkolnicka, D., Farnworth, S.L., Lucendo-Villarin, B., Storck, C., Zhou, W., Iredale, J.P., Flint, O., and Hay, D.C. (2014). Accurate prediction of drug-induced liver injury using stem cell-derived populations. Stem Cells Transl. Med. *3*, 141–148.

Tahamtani, Y., Azarnia, M., Farrokhi, A., Sharifi-Zarchi, A., Aghdami, N., and Baharvand, H. (2013). Treatment of human embryonic stem cells with different combinations of priming and inducing factors toward definitive endoderm. Stem Cells Dev. *22*, 1419–1432.

Tan, J.Y., Sriram, G., Rufaihah, A.J., Neoh, K.G., and Cao, T. (2013). Efficient derivation of lateral plate and paraxial mesoderm subtypes from human embryonic stem cells through GSKi-mediated differentiation. Stem Cells Dev. *22*, 1893–1906.

Taylor, J., Wilmut, I., and Sullivan, G. (2010). What are the limits to cell plasticity? Cell Res. *20*, 502–503.

Touboul, T., Hannan, N.R.F., Corbineau, S., Martinez, A., Martinet, C., Branchereau, S., Mainot, S., Strick-Marchand, H., Pedersen, R., Di Santo, J., et al. (2010). Generation of functional hepatocytes from human embryonic stem cells under chemically defined conditions that recapitulate liver development. Hepatology *51*, 1754–1765.

**Stem Cell Reports**

**Supplemental Information**

# Small-Molecule-Driven Hepatocyte Differentiation of Human Pluripotent Stem Cells

**Richard Siller, Sebastian Greenhough, Elena Naumovska, and Gareth J. Sullivan**

Supplemental Data

**Figure S1. Related to Figure 1. (Sullivan)**

A

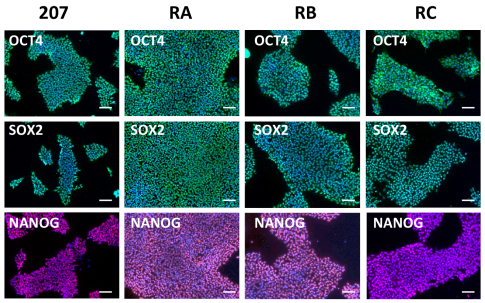


B

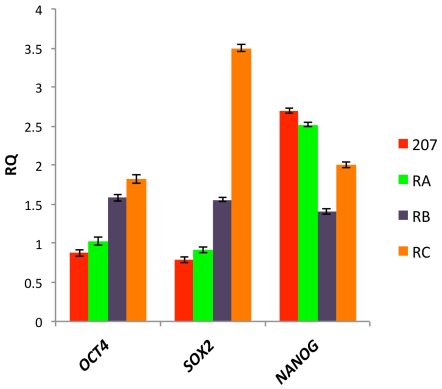


C

| 1 Day | 1 Day | 5 Days | 10 Days |
|---|---|---|---|
| RPMI-B27<br>+/- INSULIN<br>+ 3-4 μM<br>CHIR99021 | RPMI-B27 | KOSR<br>+ 1% DMSO | L-15<br>+ 100 nM Dihexa<br>+ 100 nM DEX |

D

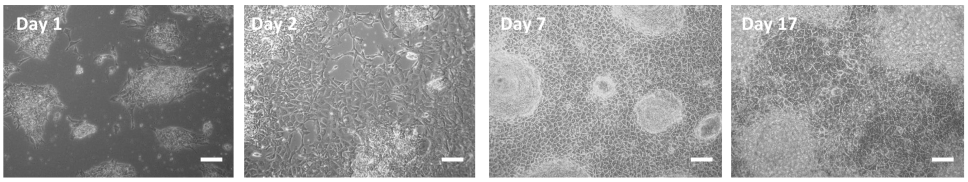

**Figure S2. Related to Figure 2. (Sullivan)**

A

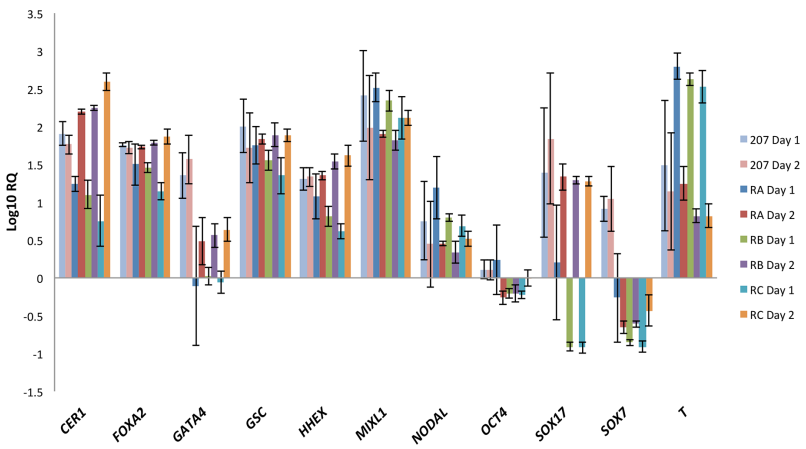


B

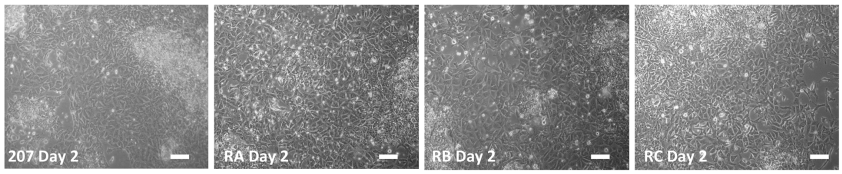


C

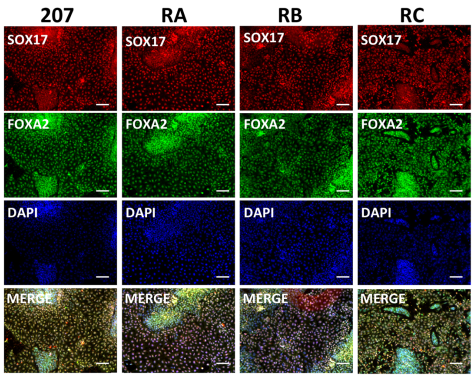


D

| Line | FOXA2 | SOX17 |
|---|---|---|
| 207 | 81.9% +/- 8.7 | 82.8% +/- 7.4 |
| RA | 84.2% +/- 7.2 | 81.3% +/- 6.9 |
| RB | 82.1% +/- 8.0 | 82.9% +/- 6.8 |
| RC | 82.2% +/- 5.1 | 79.9% +/- 7.8 |

**Figure S3. Related to Figure 3. (Sullivan)**

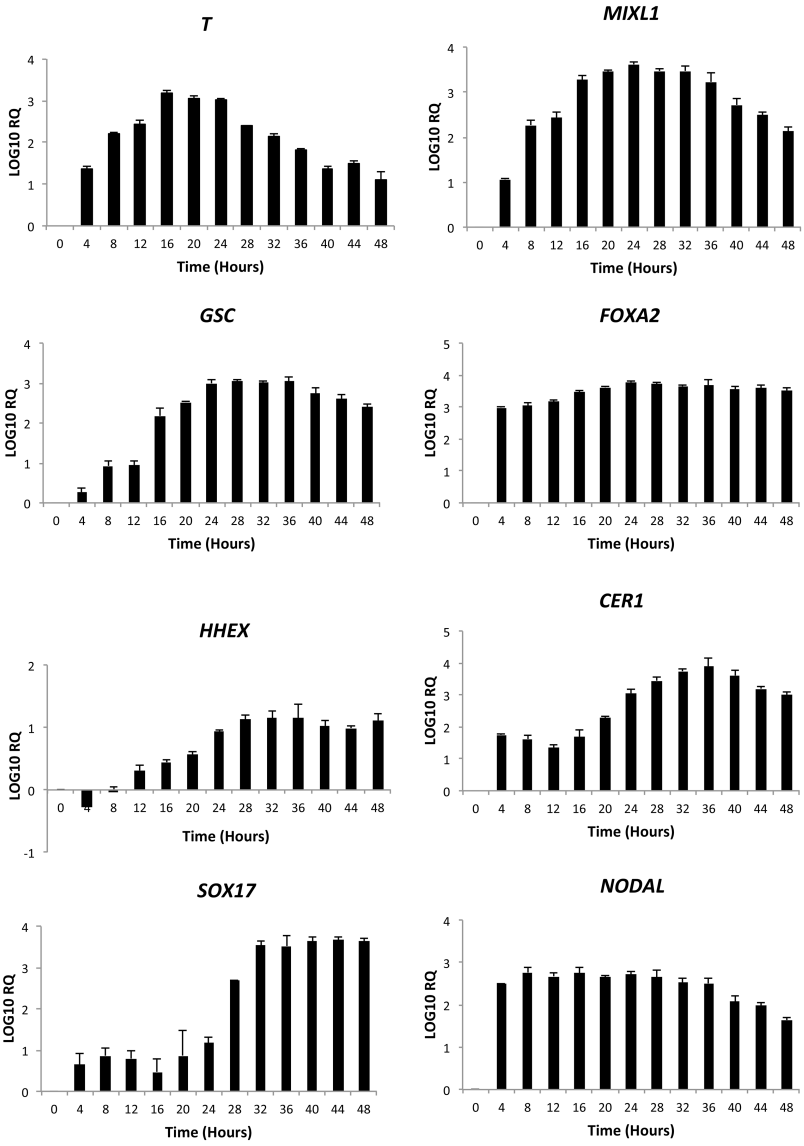

**Figure S4. Related to Figure 4. (Sullivan)**

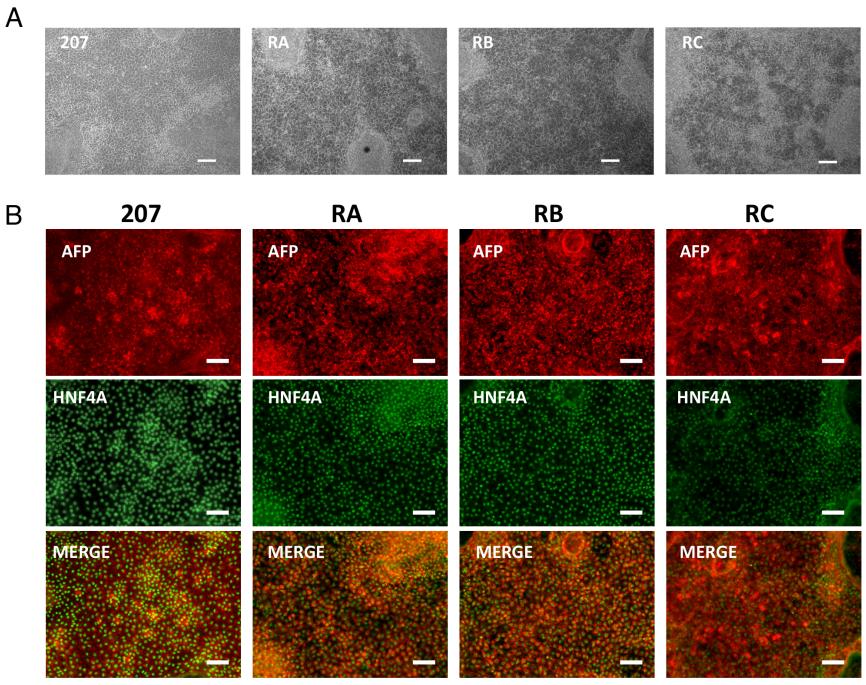


C

| Line | HNF4A / AFP |
|---|---|
| 207 | 89.2% +/- 2.4 |
| RA | 86.1% +/- 3.6 |
| RB | 87.8% +/- 3.1 |
| RC | 88.7% +/- 2.7 |

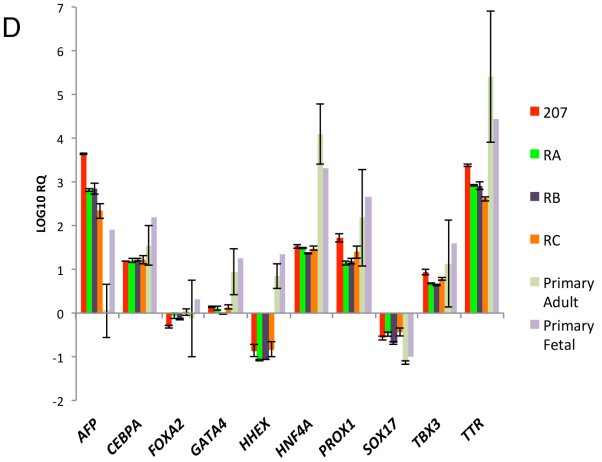

**Figure S5. Related to Figure 5. (Sullivan)**

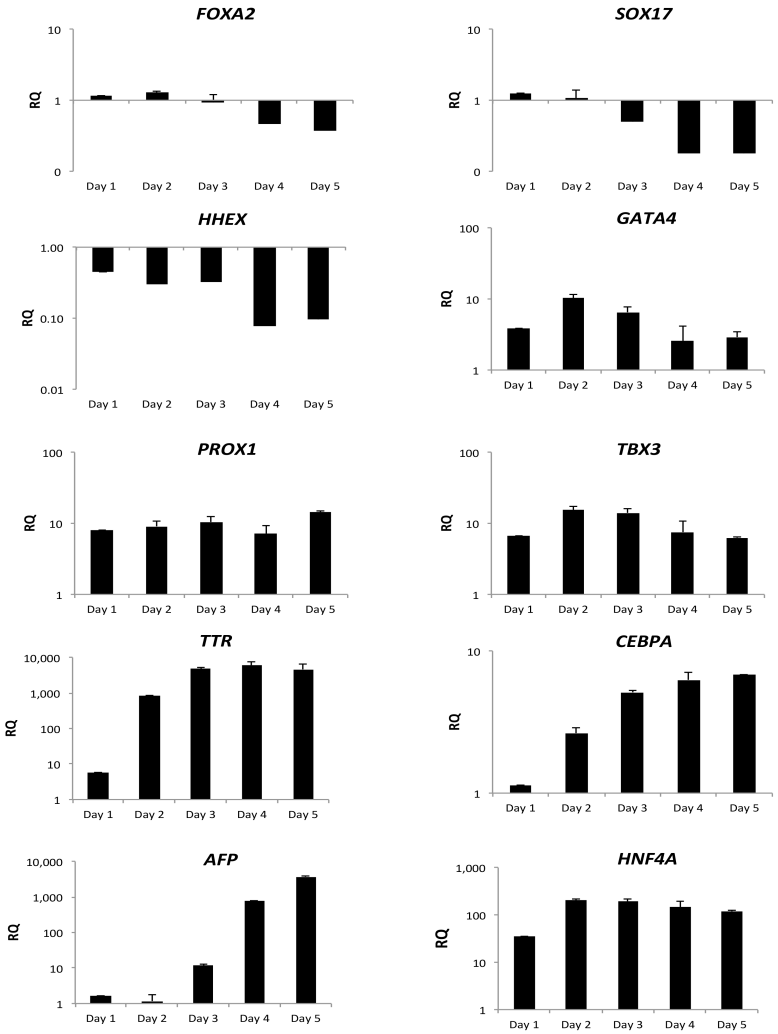

**Figure S6. Related to Figure 6. (Sullivan)**

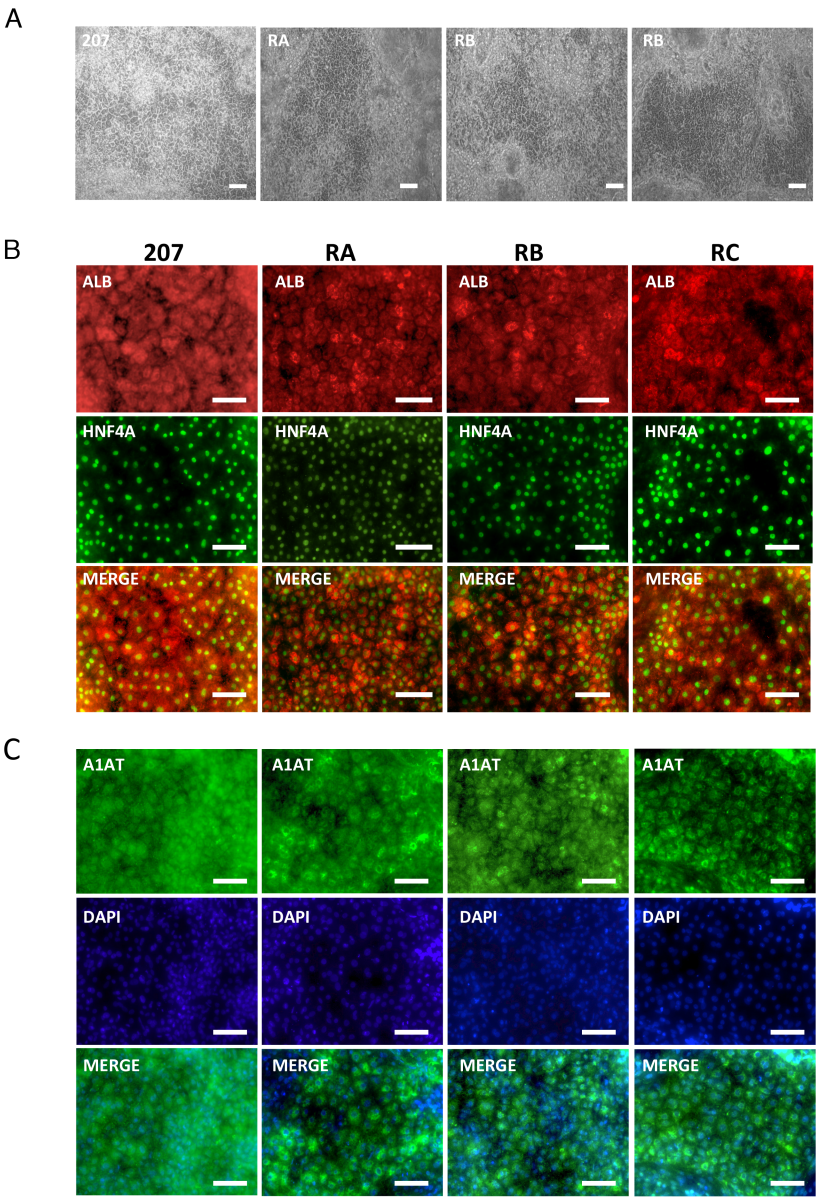

**Figure S7. Related to Figure 7. (Sullivan)**

A

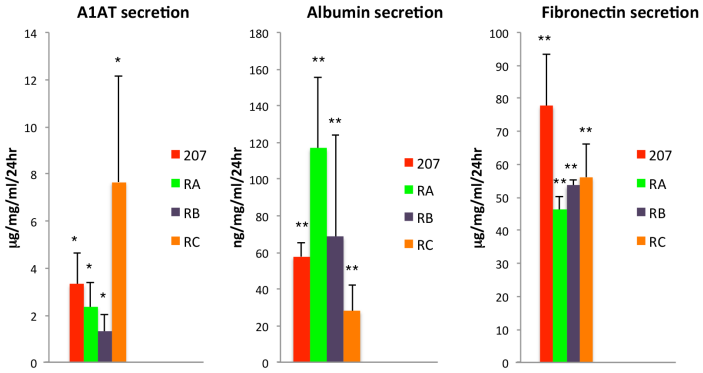


B

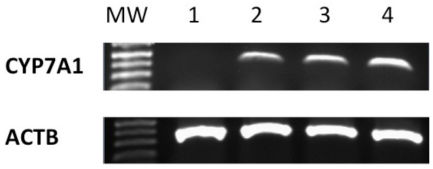


C

| Line | ALB / HNF4 | A1AT |
|---|---|---|
| 207 | 79.4% +/- 7.2 | 91.9% +/- 2.8 |
| RA | 72.1% +/- 6.9 | 90.1% +/- 1.4 |
| RB | 73.8% +/- 7.9 | 92.7% +/- 2.9 |
| RC | 75.9% +/- 8.3 | 88.7% +/- 4.6 |

D

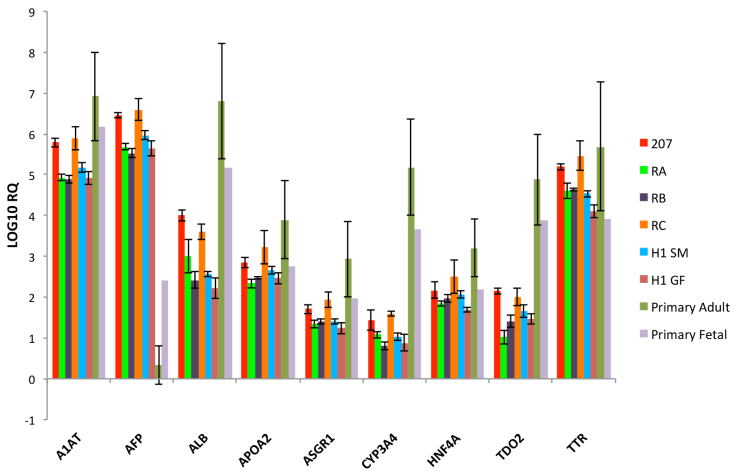

***Figure S1. hiPSC Characterisation and differentiation scheme.*** A) Expression of OCT4, SOX2, and NANOG, imaged using fluorescent microscopy. Cell line identity is indicated at the head of each column. Scale bars = 100 μm. B) Gene expression for key pluripotency genes *OCT4* (*POU5F1*), *SOX2*, and *NANOG* by RT-qPCR, normalised to H1 undifferentiated control. C) Schematic of the small molecule differentiation process on other pluripotent stem cell lines showing optimisation of CHIR99021 concentrations and base media compositions (+/-INS). D) Representative images of morphology throughout the differentiation procedure on Detroit hiPSC lines. Imaged using phase contrast microscopy. Scale bars = 100 μm.

***Figure S2. Characterisation of Phase I differentiation on multiple pluripotent lines***. A) Gene expression changes during Phase I of differentiation assessed by RT-qPCR. All lines were differentiated using RPMI / B27 (minus insulin) supplemented with 4 μM CHIR99021. Cells were collected at days 1 and 2 and analysed by TaqMan. Data presented as the mean of 3 independent experiments; error bars represent standard deviation. B) Typical morphology of small molecule derived definitive endoderm end points taken using phase contrast microscopy (10x). Line identity located bottom right corner of each plate. Scale bars = 100 μm. C) Expression of FOXA2 and SOX17 at Phase I endpoint after treatment with CHIR99021 imaged using fluorescent microscopy. Line identity located at the head of each plate. Scale bars = 100 μm. D) Efficiency of Phase I differentiation for each line was determined by counting FOXA2 positive cells and SOX17 positive cells. Efficiencies are presented as the percentage of positive cells plus or minus the standard deviation of all fields counted.

***Figure S3. Phase I 48 hour time course to assess transcriptional developmental trajectory.*** The human induced pluripotent stem cell line Detroit RA was differentiated in RPMI-B27 (minus insulin) supplemented with 4 μM CHIR99021. The expression profiles of key genes were examined to establish the dynamics of the differentiation process. We monitored developmentally relevant markers of primitive streak (*T, MIXL1, GSC, FOXA2*), mesendoderm (*T*, *FOXA2*), and definitive endoderm (*HHEX, CER1, SOX17, FOXA2*). Cells were collected for analysis every 4 hours for 48 hours (Phase I - DE stage). Data presented as the mean of 3 independent experiments; error bars represent standard deviation. The X-axis represents the time (in hours) after the start of differentiation. The Y-axis represents the Log10 RQ values from the TaqMan analysis.

***Figure S4. Characterisation of Phase II on multiple pluripotent lines - hepatic specification.*** A) Typical morphology observed at Phase II endpoint, photographed using phase contrast microscopy at 10x. Line identity located top left corner of each plate. Scale bars = 100 μM. B) Expression of AFP and HNF4A at Phase II endpoint of small molecule treated cells, imaged using fluorescent microscopy. The line identity is above each column. Scale bars = 100 μM. C) Efficiency of Phase II differentiation was determined for each line by counting HNF4A and AFP double positive cells. Efficiencies are presented as the percentage of positive cells plus or minus the standard deviation of all fields counted. D) Expression of *AFP, CEBPA, FOXA2, GATA4, HHEX, HNF4A, PROX1, SOX17, TBX3, and TTR* at Phase II endpoint, measured by TaqMan. Normalised to *ACTB* and small molecule derived definitive endoderm. Data presented as the mean of 3 independent experiments; error bars represent standard deviation.

***Figure S5. Phase II 5 day time course.*** The human induced pluripotent stem cell line Detroit RA was differentiated to definitive endoderm using the small molecule protocol. Definitive endoderm was treated with 1% DMSO to differentiate to hepatic progenitors. Cells were collected every 24 hours and gene expression of developmentally relevant hepatic markers was assessed. Data presented as the mean of 3 independent experiments; error bars represent standard deviation. The X axis represents the time (in days) after definitive endoderm. The Y axis represents the RQ values from the TaqMan analysis.

***Figure S6. Characterisation of Phase III differentiation to hepatocyte like cells: Morphology and immunofluorescence***. A) Morphology of hESC line 207, hiPSC lines Detroit RA, RB and RC at small molecule protocol endpoint (day 17), taken using phase contrast microscopy at 10x. Line identity located top left of each plate Scale bars = 100 μm. B) Expression of albumin and HNF4A at protocol endpoint imaged using fluorescent microscopy. Line identity located at the head of each plate. Scale bars = 100 μm. C) Expression of alpha-1-antitrypsin at protocol endpoints, imaged using fluorescent microscopy. Scale bars = 100 μm.

***Figure S7. Characterisation of Phase III derived hepatocyte like cells: RT-qPCR and functional analysis.*** A) Serum protein secretion at endpoint of small molecule protocol for all lines. Data is presented as the mean of 3 independent experiments; error bars represent standard deviation. *$p < 0.02$, **$p < 0.003$ compared to control. B) Assessment of RT-PCR of *CYP7A1* gene expression of hiPSC derived smHLCs. Lane1 = hESC H1 control, lane 2= Detroit RA, Lane 3 = Detroit RB, Lane 4 = Detroit RC day 17 smHLCs *CYP7A1* expression, lower panel = *ACTB* loading control. C) Efficiency of Phase III differentiation, determined by counting albumin and HNF4A double positive cells and A1AT positive cells. Efficiencies are presented as the percentage of positive cells plus or minus the standard deviation of all fields counted. D) Expression of *A1AT (SERPINA1),*

*AFP, ALB, APOA2, ASGR1, CYP3A4, HNF4A, TDO2 and TTR* at endpoint of small molecule protocol, as well as growth factor derived HLCs, primary adult and fetal hepatocyte controls, as measured by TaqMan. All normalised to *ACTB* small molecule derived definitive endoderm. Data is presented as the mean of 3 independent experiments; error bars represent standard deviation. Only 1 primary fetal control was run therefore no error bars present.

***Table S1. Primer details for RT - qPCR***

***Table S2. Antibody details for immunofluorescence***

***Table S3. Primer sequence details***

***Table S4. Small molecule details***

Table S1.

| Target | Manufacturer | Reference |
|---|---|---|
| ***OCT4*** | Life Technologies | Hs00999634_gH |
| ***SOX2*** | Life Technologies | Hs01053049_s1 |
| ***NANOG*** | Life Technologies | Hs04260366_g1 |
| ***NODAL*** | Life Technologies | Hs00415443_m1 |
| ***MIXL1*** | Life Technologies | Hs00430824_g1 |
| ***T*** | Life Technologies | Hs00610080_m1 |
| ***GSC*** | Life Technologies | Hs00906630_g1 |
| ***SOX7*** | Life Technologies | Hs00846731_s1 |
| ***GATA4*** | Life Technologies | Hs00171403_m1 |
| ***FOXA2*** | Life Technologies | Hs00232764_m1 |
| ***SOX17*** | Life Technologies | Hs00751752_s1 |
| ***HHEX*** | Life Technologies | Hs00242160_m1 |
| ***CER1*** | Life Technologies | Hs00193796_m1 |
| ***AFP*** | Life Technologies | Hs00173490_m1 |
| ***HNF4A*** | Life Technologies | Hs00230853_m1 |
| ***CEBPA*** | Life Technologies | Hs 00269972_s1 |
| ***PROX1*** | Life Technologies | Hs00896294_m1 |
| ***TBX3*** | Life Technologies | Hs00195612_m1 |
| ***ASGR1*** | Life Technologies | Hs01005019_m1 |
| ***TDO2*** | Life Technologies | Hs00199611_m1 |
| ***APOA2*** | Life Technologies | Hs00952079_g1 |
| ***ALB*** | Life Technologies | Hs00910225_m1 |
| ***CYP3A4*** | Life Technologies | Hs00604506_m1 |
| ***TTR*** | Life Technologies | Hs00174914_m1 |
| ***A1AT (SERPINA1)*** | Life Technologies | Hs01097800_m1 |
| ***ACTB*** | Life Technologies | N/A |

Table S2.

| Target | Manufacturer | Catalogue Number | Species | Dilution |
|---|---|---|---|---|
| **OCT4** | **Stemgent** | **09-0023** | **Rabbit** | **1:100** |
| **SOX2** | **Stemgent** | **09-0024** | **Rabbit** | **1:100** |
| **NANOG** | **Stemgent** | **09-0020** | **Rabbit** | **1:100** |
| **FOXA2** | **AbCam** | **ab40874** | **Rabbit** | **1:1000** |
| **SOX17** | **AbCam** | **ab84990** | **Mouse** | **1:100** |
| **AFP** | **Sigma-Aldrich** | **A8452** | **Mouse** | **1:500** |
| **HNF4A** | **Santa Cruz** | **sc8987** | **Rabbit** | **1:100** |
| **ALBUMIN** | **Sigma-Aldrich** | **A6684** | **Mouse** | **1:500** |
| **Alpha-1-antitrypsin** | **Santa Cruz** | **sc30121** | **Rabbit** | **1:50** |
| **Alexaflour 488 anti rabbit** | **Life Technologies** | **A21206** | **Donkey** | **1:400** |
| **Alexafluor 488 anti mouse** | **Life Technologies** | **A11059** | **Rabbit** | **1:400** |
| **Alexafluor 594 anti mouse** | **Life Technologies** | **A11005** | **Goat** | **1:400** |

Table S3.

| **Target** | **Forward sequence 5´-3´** | **Reverse sequence 5´-3´** |
|---|---|---|
| ***ACTB*** | TCACCACCACGGCCGAGCG | TCTCCTTCTGCATCCTGTCG |
| ***CYP7A1*** | CTGCCAATCCTCTTGAGTTCC | ACTCGGTAGCAGAAAGAATACATC |

Table S4.

| Name | Source | Purity | Solvent | Phase of protocol used | Final concentration used |
|---|---|---|---|---|---|
| CHIR99021 | STEMGENT | >95% | DMSO | Phase I | 3-4 μM |
| BIO | Tocris | >98% | DMSO | Alternative Phase I | 1 μM |
| DMSO | Sigma-Aldrich | ≥99.9% | N/A | Phase II | 1% by volume |
| Dexamethasone | Sigma-Aldrich | ≥97% | DMSO | Phase III | 100 nM |
| Dihexa | Kind gift of Prof. Joseph Harding Washing State University | 93% | DMSO | Phase III | 100 nM |

## Supplemental Experimental Procedures

***Human induced pluripotent stem cell derivation and characterisation.***

Detroit 551 fibroblasts were obtained from the American Type Culture Collection (ATCC CCL-110). hOCT4, hSOX2, hcMYC, and hKLF4, retrovirus viral particles were generated by Vectalys and transduced at an MOI of 5 as described by Vallier and colleagues (Vallier et al., 2009). On appearance, hiPSCs were picked and expanded feeder free on Matrigel (Sigma-Aldrich) in E8 Medium (Life Technologies). We verified the iPSC lines expressed human embryonic stem cell markers by immunocytochemistry for NANOG, SOX2 and OCT4 expression (Figure S1A). We also used RT-qPCR to confirm that iPSCs expressed *NANOG, SOX2* and *OCT4* (Figure S1B) and that they had silenced the exogenous genes that were used for reprograming (data not shown). We karyotyped the iPSC lines using KaryoLite BoBs (Perkin Elmer) and demonstrated they were normal (performed by Finnish Microarray and Sequencing Centre (FMSC)). Finally we demonstrated that the derived hiPSCs were able to generate all three germ layers: ectoderm (neurons), mesoderm (cardiomyocytes) and endoderm (hepatocytes) (data not shown), indicating that the iPSCs generated are pluripotent.

***RNA isolation and RT-qPCR***.

RNA was isolated from cells using TRIzol according to manufacturer's instructions and quantified using a spectrophotometer (NanoDrop). cDNA was prepared using the High Capacity Reverse Transcription kit and a thermal cycler (both from Life Technologies). RT-qPCR was performed using a TaqMan ViiA7 Real Time PCR System with TaqMan Gene Expression Master Mix (Life Technologies). TaqMan assays were used to assess markers of interest and *ACTB* was used as an endogenous control (Life Technologies); see Table S1 for details. Expression levels were quantified relative to *ACTB* and normalised to undifferentiated pluripotent control samples or definitive endoderm cells

as specified. Results are shown as the mean of 3 independent experiments; error bars represent standard deviation.

***Immunofluorescence***.

Cells were washed with PBS before being fixed with a 10 minute treatment of ice cold methanol. Fixed cells were washed in 0.1% PBS-T: PBS containing 0.1% Tween 20 (Sigma-Aldrich). Cells were blocked for 1 hour in 10% normal goat serum (Life Technologies) made up in 0.1% PBS-T. Cells were then washed twice before being treated with primary antibodies overnight at 4°C; see Table S2 for antibody details. All primary antibodies were made up in 1% normal goat serum in 0.1% PBS-T. Secondary antibody only controls were also included. Following primary incubations, all cells were washed twice and treated with Alexafluor secondary antibodies (Life Technologies) for 1 hour at room temperature. The secondary antibodies were made up in PBS. Cells were then washed twice in PBS-T and twice in PBS before being mounted using Fluoroshield with DAPI (Sigma-Aldrich) and glass coverslips. Cells were imaged using a Zeiss Observer Fluorescence Microscope and Axiovision imaging software. The scale bars represent 100 μm.

***Glycogen storage, periodic acid–Schiff staining assay and uptake of indocyanine green.***

In order to assess glycogen storage, differentiated cells were fixed and treated with a periodic acid-Schiff staining kit (Sigma-Aldrich) in accordance with manufacturer's instructions and imaged using a Zeiss phase contrast microscope and ZEN software. The scale bars represent 100 μm. We also assessed the cellular uptake of indocyanine green, briefly, ICG (Sigma-Aldrich) was reconstituted in water and used at a final concentration of 1 mg/ml. Cells were incubated in media supplemented with ICG for 1 hour, the cells

were then washed with PBS and imaged using a Zeiss phase contrast microscope and ZEN software.

***Cytochrome P450 Induction and analysis.***

Induction of cytochrome P450 activity was assessed in both small molecule and growth factor derived HLCs. CYP1A2 activity was detected using the P450-Glo CYP1A2 Induction/Inhibition Assay kit (Promega, Cat. no. V8422). CYP3A4 activity was detected using the P450-Glo CYP3A4 (Luciferin-PFBE) Cell-Based/Biochemical Assay (Promega V8902). Assays were performed according to the manufacturer's instructions for non-lytic P450-Glo assays using cultured cells in monolayers. Cytochrome P450 inductions were performed using the following inducers: for CYP3A4, Rifampicin (25 μM) and CYP1A2, Omeprazole (100 μM) (both purchased from Sigma). Briefly, cells were cultured to day 20 of the differentiation protocol and Rifampicin or Omeprazole was added to L-15 culture medium, which was formulated as described above, but without dexamethasone or hydrocortisone. Medium was replaced daily for 72 hours. After 72 hours, the cells were washed 4 times with PBS (calcium/ magnesium free) and then assayed. Briefly, for CYP1A2 the substrate Luciferin-1A2 was diluted to 6 μM in PBS (calcium/ magnesium free) containing 3 mM freshly prepared salicylamide (Sigma). The Luciferin substrate was added to each well (1 ml per well of a 6 well plate), and incubated for 60 minutes followed by detection. For CYP3A4, the substrate Luciferin-PFBE was diluted in L-15 culture medium (formulated as described above), to a final concentration of 50 μM. After washing the cells, 1 mL of Luciferin-PFBE containing media was added to each well and incubated for 4 hours followed by detection. We assessed basal activity as above with the omission of inducers. In addition, no cell media controls were included. Finally as a negative control, the pluripotent hESC line H1 was assayed for CYP activity as described above. All data was normalised to total protein content in each well. Data is presented as the mean values of 6 independent experiments; error bars represent standard deviation.

***Serum protein production***.

Cells were incubated for 24 hours in 1 ml of media. ELISA kits were then used to detect human albumin (Alpha Diagnostics), fibronectin (AbCam) and alpha-1-antitrypsin (AbCam) in the supernatants according to manufacturer's instructions. Negative control incubations without cells were included as blanks. Results are normalised to protein weight, and given as the mean of 3 independent experiments; error bars represent standard deviation.

***Protein extraction and quantification***.

Cells were lysed in 250 µl of SUMO buffer containing 2% sodium dodecyl sulphate (SDS), 50 mM Tris (pH 8), 1 mM EDTA and 10 mM iodoacetamide (Sigma-Aldrich) for 5 minutes at room temperature. Total protein was quantified using a BCA Assay Kit (Pierce) and an absorbance plate reader (Tecan).

***PCR and gel electrophoresis.***

PCR was carried out using AmpliTaq Gold 360 Master Mix (Life Technologies) supplemented with the relevant oligonucleotide pairs. All assays were run against an *ACTB* control to ensure equivalent amounts of input cDNA; in all cases 5 ng of input cDNA was used. The oligonucleotide sequences are provided in the Table S3. The PCR products were resolved using agarose gel electrophoresis.

***Cell Counting.***

Immuno-stained cells were quantified for expression of stage specific markers by manual counting. For Phase I, FOXA2 and SOX17 were counted separately. For Phase II, cells were scored positively if the nucleus was stained for HNF4A and the cytoplasm was stained for AFP. For Phase III, cells were scored positively if the nucleus was HNF4A

positive and the cytoplasm was ALB positive. Phase III cells were also quantified for AFP and A1AT staining and were counted as positive if the cytoplasm was stained. In all cases, 3D areas in the image were excluded due to difficulties in counting the nuclei. A minimum of 10 fields of view were quantified, with a minimum of 250 cells counted per field of view. Percentages are presented as the average of all field quantifications, plus or minus the standard deviation across all fields.

**Statistical Analysis**.

Results were evaluated by performing t tests. $p < 0.09$ was determined significant.

# Supplemental References

Vallier, L., Touboul, T., Brown, S., Cho, C., Bilican, B., Alexander, M., Cedervall, J., Chandran, S., Ahrlund-Richter, L., Weber, A., Pedersen, R.A., 2009. Signaling pathways controlling pluripotency and early cell fate decisions of human induced pluripotent stem cells. Stem Cells 27, 2655–2666. doi:10.1002/stem.199